Studies on the decontamination methods for restoring biocompatibility of contaminated titanium surfaces

2018

Graduate School of Dentistry
Health Sciences University of Hokkaido

Yuki ICHIOKA

Abstract

Surface decontamination methods for rejuvenating or restoring the biocompatibility of the contaminated titanium surfaces by the adsorption of atmospheric organic impurities or bacterial plaque, respectively, has investigated in the current thesis of studies. First of all, in study I, the effects of chemical treatment using 5% sodium hypochlorite (NaOCl) solution to the aged titanium surfaces, which contaminated by atmospheric organic impurities, were evaluated. The aged titanium disks were immersed in NaOCl solution for 24 hours. As a control, the disk immersed in distilled water for 24 hours was employed. XPS assay demonstrated that the atmospheric organic impurities on the untreated titanium were removed and the amount of hydroxyl group was increased after NaOCl treatment. The NaOCl treatment substantially converted the titanium surface to superhydrophilic ($\theta < 5^{\circ}$), which resulted in increasing the number of attached cells and enhancing the cell spreading on the NaOCl treated surfaces. These results proposed that bio-functionalization of the titanium surface can be achieved by treatment with NaOCl.

Secondly, in study II, the cytocompatibility of experimentally contaminated titanium disks, using a *Streptococcus gordonii* biofilm, after chemical treatment with aqua alkaline electrolyzed water (AAEW) as an adjunctive to air-abrasive debridement were assessed. The contaminated disks were treated with air-abrasion and immersion in either 0.9% NaCl (Air + NaCl), 0.05% AAEW (Air + AAEW), or 3% H_2O_2 (Air + H_2O_2). The efficacy of biofilm removal, magnitude of initial cytocompatibility and surface chemical properties were determined. In all treatment groups, biofilms were observed to be completely removed. However, the data showed discrepancies for cell affinities among treatment groups, whereby: i) the number of cells attached to Air + AAEW was approximately 2-fold greater than that to Air + NaCl; and ii) cell spreading was enhanced on Air + AAEW compared with Air + NaCl or Air + H_2O_2. When evaluated by XPS, these discrepancies could be attributed to sufficient removal of organic-nitrogen deposits at the same magnitude as the pristine surface following Air + AAEW treatment. The present study clarifies that chemical surface treatment with AAEW as an adjunctive to air-abrasive debridement may be beneficial in achieving re-osseointegration.

Table of Contents

Introduction

Implant dentistry is now a widely accepted treatment in the world. Although no reliable documentation exists, it has been estimated that approximately 12 million osseointegrated oral implants are placed annually in a global perspective (Albrektsson et al., 2014). A dental implant fixture generally made of pure titanium or titanium alloys integrates with the surrounding bone directly. The formation of a direct interface between an implant and bone without intervening soft tissue is termed "osseointegration" (Albrektsson et al., 1981). Osseointegration was discovered when working with implants in research animals at the laboratory of the Göteborg University (Brånemark, 1977). The discovery was made around 1962, and it has meant an enormous advancement for clinical treatment of oral implants (Albrektsson et al., 2017). Since the discovery in 1962, ossteointegrated titanium implant have constituted a safe, accepted and commonly applied method (E Jung et al., 2012; Pjetursson et al., 2012). However, we have to realize that two kinds of contamination to the titanium surface which directly induced the reduction of biologic capability have been reported separately.

The problems caused by the contaminations are known as **"Biological Aging"** and **"Peri-implantitis"**.

1. Biological aging and chemical surface treatment (Study I)

1-1) What is biological aging of titanium?

Biological aging defines as a natural time-dependent degradation of osseointegration capability of titanium. In 2009, Att et al. reported that biocompatibility of titanium implant degraded over time after surface processing. The biological aging is associated with an inevitable occurrence of progressive contamination of the titanium surfaces by organic impurities, such as polycarbonyls and hydrocarbons quickly adsorbed on the titanium implant surface from the atmosphere, water, and cleaning solutions (Kilpadi et al., 2000; Serro & Saramago, 2003).

1-2) Are there evidences that titanium surfaces manifest biological changes over time during their storage?

The aging of titanium reduces the initial behavior and response of osteoblasts, such as the migration, attachment, and proliferation of the cell (Lee & Ogawa, 2012). Some studies revealed that these degrades were attributed to the age-related impaired bioactivity of the implants, defined as the biological aging of titanium (Att et al., 2009; Att & Ogawa, 2012; Lee & Ogawa, 2012). Additionally, the age-induced reduction of these *in-vitro* cell behavior was observed on various surface topographies not only just acid-etch-created microtopography, but machined and sandblasted surfaces (Att et al., 2009; Suzuki et al., 2009). Minamikawa et al. (2016) evaluated the biological capability of titanium during six months of aging, with a particular focus on its interaction with osteogenic cells. The authors demonstrated that the degradation of the biological capability of titanium was time-dependent and progressed up to 6 months. In *in-vivo* studies, implant biomechanical push-in test or bone-implant contact (%) in a rat model has been widely used to assess the osseointegration capability of various titanium surfaces and different healing capacities of the host (Weinlaender et al., 1992; Ozawa et al., 2002; Ogawa & Nishimura, 2003; Att et al., 2009; Ueno et al., 2010a; Ueno et al., 2010b). For instance, Att et al, (2009) compared the strength of osseointegration in the acid-etched implants with different storage time of 3 days, 2 weeks, and 4 weeks. After 2 weeks of healing, the strength of osseointegration, measured by the push-in value, for the new implants was 37 N, whereas it was 36, 24, and 16 N for 3-day-old implants, 2-week-old implants, and 4-week-old implants, respectively. Bone histomorphometry demonstrated that the percentage of bone-implant contact for the new implants (approximately 70% at 2 weeks healing and 90% at 4 weeks healing) was consistently greater than that for the 4-week-old implants (approximately 30% at 2 weeks healing and 60% at 4 weeks healing). Taken together, the phenomenon of biological aging seem to be cause the quality of osseointegration to decrease markedly. There is, hence, a need to improve its bioactivity for a therapeutic and experimental purpose.

1-3) A new approach to rejuvenate the aged titanium with NaOCl solution

Various surface treatment methods have been suggested in order to solve this phenomenon; ultraviolet light treatment (Aita et al., 2009), gamma ray treatment (Ueno

et al., 2012), alkali and heat treatment (Nishiguchi et al., 1999), atmospheric pressure plasma jet (Duske et al., 2012), and cold-plasma technique (Yoshinari et al., 2011). Aita et al. (2009) reported that the creation of highly bioactive and osteoconductive titanium surfaces was achieved via ultraviolet (UV) light treatment. However, these surface treatments are costly and required special devices. In study I, the new approach to the biological aging with sodium hypochlorite (NaOCl) solutions has been proposed. NaOCl is a typical strong oxidant and commonly used for irrigation in endodontics. The merits of NaOCl treatment are low cost, no special appurtenances and have a possibility of applications for nanoporous surface due to its liquid nature. Kono et al. (2015) performed a series of animal studies and reported that the strength of bone-titanium integration for polished and acid-etched surfaces with the NaOCl treatment at the early-stage of healing (2 weeks) increased 1.3 times and 1.4 times than those of the untreated polished and untreated acid-etched titanium, respectively, when evaluated with push-in tests. Moreover, in histological images of peri-implant tissue at 2 weeks, bone formation occurred more extensively around the NaOCl-treated implants than that around the untreated implants. These results showed that NaOCl pretreatment enhanced the osseointegration capability of titanium, indicating successful NaOCl-mediated biofunctionalization of titanium implant surface. The aim of this study was, thus, to evaluate the NaOCl-mediated biofunctionalization of titanium surface by surface characterization using an X-ray photoelectron spectrometer (XPS) and an automatic contact angle measuring device. *In-vitro* protein adsorption assay and cell culture experiments were also done. In addition, the underlying mechanisms of NaOCl-mediated biofunctionalization of titanium were also elucidated considering the interactions of ClO^- with organic contaminants adsorbed on the titanium surface as well as time-dependent biological degradation process of titanium.

2. Peri-implantitis and surface decontamination procedure (Study II)

2-1) What is peri-implantitis? (Study II)

A consensus report from World Workshop on Classification of Periodontal and Peri-implant Diseases and Conditions 2017 stated that peri-implantitis is a

plaque-associated pathological condition occurring in tissues around dental implants, characterized by inflammation in the peri-implant mucosa and subsequent progressive loss of supporting bone (Berglundh et al., 2018). Bacterial biofilm has been identified as the main etiological factor of peri-implantitis. Clinical studies have shown that bacterial biofilm development initiates inflammation at implant sites which, if left untreated, can progress into peri-implantitis (Schwarz et al., 2014; Jepsen et al., 2015; Renvert & Polyzois, 2015). In a systematic review, it was stated that the estimated prevalence of peri-implantitis is 22% (Derks & Tomasi, 2015). It has, therefore, become widely recognized as a major and increasing problem in dentistry. There is significant interest in establishing effective treatment modalities to resolve soft tissue inflammation and, thereby, preventing further bone loss.

2-2) Treatment of peri-implantitis

The primary goals of treatment of peri-implantitis are resolution of tissue inflammation and, subsequently, the prevention of further marginal bone loss. Moreover, the ultimate goals are represented as supra crestal tissue re-attachment and re-osseointegration of the exposed implant surface. As peri-implantitis are driven by plaque, anti-infective treatment has been the principal treatment modality for peri-implantitis. In most cases, surgical access is required to allow for proper decontamination of the affected implant surfaces. Thus, following the surgical exposure of the diseased implant surfaces, mechanical, chemical, and/or photodynamic measures have been used in the attempt to eliminate bacterial infection, possibly rendering the surface conducive to re-osseointegration and bone regeneration (Claffey et al., 2008).

2-3) What is the key factor for achieving substantial re-osseointegration?

Re-osseointegration occurs based on cell adhesion to titanium oxide film. Surface characteristics of implant, whether their topography, chemistry or surface energy, play an essential part in osteoblast adhesion on implant surface (Yoshinari et al., 2002; Feng et al., 2003; Ogawa & Nishimura, 2003; Att et al., 2009; Att & Ogawa, 2012; Lee & Ogawa, 2012; Yamamura et al., 2015). Thus attachment, adhesion and spreading belong

to the first phase of cell/oxide film interactions and the quality of this first phase will influence the cell's capacity to proliferate and to differentiate itself on contact with the implant surface. As the main etiology of peri-implantitis refers to bacterial biofilm accumulation, there is no doubt that the bacterial biofilm removal is strategy for the management of peri-implant diseases. However, even if the bacterial biofilm could be completely removed, there is some doubt whether the titanium surface was reestablished high biocompatibility as same as pristine implant. Renvert et al. (2009) concluded that implant surface characteristics may influence the degree of re-osseointegration. In addition, Persson et al. (2001) used a canine model to determine whether titanium surface quality is a decisive factor for osseointegration and re-osseointegration. The authors used a specially designed implant system in which the implant body consisted of upper and lower components, so the upper component could be replaced. Using this approach, the authors demonstrated that significant re-osseointegration failed to occur adjacent to implant surfaces exposed to bacterial contamination followed by mechanical cleaning of the surfaces using cotton pellets soaked in saline. However, integration consistently occurred at sites where the exposed upper implant component was replaced with a pristine component following surgical debridement in the infected lesion. This result suggests that the success of re-osseointegration depends on reestablishment of the titanium surface properties to a pristine state during surgical treatment of peri-implantitis.

Techniques to treat peri-implantitis with re-osseointegration and bone regeneration are under investigation. Although various methods have been advocated, including air powder abrasion, saline wash, citric acid treatment, laser therapy, peroxide treatment, ultrasonic and manual debridement, and application of topical medication, a gold-standard is yet to be identified to ensure re-osseointegration (Claffey et al., 2008). Al-Hashedi et al. (2017) compared the effect of four mechanical decontamination methods (metal and plastic curettes, titanium brushes and yttrium aluminium and garnet (Er: YAG) laser) on the chemical properties of titanium surfaces. Although titanium brushes achieved greater elimination of bacteria and organic contaminants compared with curettes and Er: YAG laser, none of the methods were able to restore the original

surface chemical properties. Consequently, following surgical exposure of the contaminated implant surface, the use of mechanical, chemical, or photodynamic measures, and the combination of all three, are under consideration to eliminate bacterial infection, resolve inflammation and render the surface conducive to re-osseointegration and bone regeneration (Claffey et al., 2008). It is preferable to modify surface properties with high compatibility for the attachment of bone marrow-derived mesenchymal stem cells (BMSCs) for regenerative therapy applications (Persson et al., 2001; Parlar et al., 2009).

2-4) A new chemical approach to restore the surface properties for tissue integration during surgical treatment of peri-implantitis

To reestablish the ideal properties of titanium surface for re-osseointegration, the effects of hypochlorite ion (ClO^-) following air-abrasive debridement on the titanium surface are investigated in study II. It was hypothesized that surface treatment with the use of chemotherapeutic agents as an adjunctive of mechanical debridement might be beneficial for restoring implant surfaces to their original state. Aqua alkaline electrolyzed water (AAEW) containing ClO^- and hypochlorous acid (HClO) is reported to possess an oxidizing action that could be useful for decomposing and removing organic impurities on hard solid surfaces. HClO was used to decompose the surface and the study reported that the efficacy of removing the organic component was enhanced with increased ClO^- concentration by changing the pH of the HClO solution to alkaline (Urano & Fukuzaki, 2005). AAEW has since been developed and utilized within the food industry to prevent bacterial contamination (Huang et al., 2008).

3. Aims

Overall aim

To investigate the decontamination methods for restoring biocompatibility of the contaminated titanium surfaces.

Specific aims

1. To evaluate the NaOCl-mediated biofunctionalization of titanium surface by surface characterization using an X-ray photoelectron spectrometer (XPS) and an automatic contact angle measuring device. *In-vitro* protein adsorption assay and cell culture experiments were also done. In addition, the underlying mechanisms of NaOCl-mediated biofunctionalization of titanium were also elucidated. **(Study I)**
2. To evaluate the effects of chemical agents used following air-abrasive debridement on experimentally biofilm contaminated titanium surfaces with respects to changes of surface characteristics and of cytocompatibility to hBMSCs. **(Study II)**

Material & Methods

1. Processing and analysis of titanium surface

1) Titanium specimens (Study I & II)

Commercially pure grade-2 titanium disks (JIS, Japan Industrial Specification H 4600, 99.9 mass% Ti; GC Corp., Tokyo, Japan) were used.

In study I, the disks (Ø15 mm, thickness: 1.0 mm) were polished mechanically to a mirror finish using colloidal silica. The polished disks were cleaned ultrasonically in distilled deionized water for 5 minutes and then dried with oil-free compressed air. The mechanically polished pure titanium was used as the "As-polished" group. These titanium disks were stored in the dark for 2 weeks.

In study II, the disks (Ø14 mm, thickness: 3.0 mm) were polished mechanically to a machined surface using the ultra-pad (ULTRA PAD®, Buehler Ltd., Evanston, IL, USA**),** diamond polishing compound (MetaDi® II Paste) and diamond polishing suspension (MetaDi®, Mono Suspension). The polished disks were cleaned ultrasonically in distilled deionized water for 10 minutes and then dried with oil-free compressed air. The mechanically polished pure titanium was used as the "As-polished" group.

2) Bacterial strains and biofilm formation on a titanium disk (Study II)

S. gordonii ATCC 10558^T were cultured on TY agar (TY; Bacto™ tryptic soy broth and Bacto™ yeast extract) under the anaerobic conditions (N_2: CO_2: H_2, 80%: 10%: 10%) at 37˚C for three days. Single colonies of *S. gordonii* on TY agar was transferred into TY liquid culture medium. Turbidity was calibrated by measuring the absorption at OD_{660}: 0.5 (0.5×10^8 CFU/mL). 2.0 mL of portions of the bacteria suspension was transferred to 12-well polystyrene culture plate with titanium disks. The plate was incubated anaerobically (N_2: CO_2: H_2, 80%: 10%: 10%) at 37˚C for 24 hours and the growth medium was refreshed at 12 hours after the start incubation. The titanium disks after forming biofilm without any treatments were used as the biofilm contaminated group (Biofilm-contaminated).

3) Surface treatment protocols

(1) Chemical surface treatment (Study I)

The samples were divided into 3 groups; Untreated, H_2O-treated and NaOCl-treated. H_2O or NaOCl-treated surface was prepared by immersed in distilled deionized water or 5% NaOCl solution for 24 hours. NaOCl-treated disks were, then, washed gently three times with distilled deionized water. The titanium samples employed in this study were summarized in Figure 1.

(2) Decontamination procedures (Study II)

For the mechanical surface debridement, an air-flow system (Air Flow S1^R, EMS, Nyon, Switzerland) adding either amino acid glycine (Air-Flow Perio, EMS, Nyon, Switzerland) was used at maximum setting for both power and lavage. The distance between the tip of the device and the disk was set at 2 mm, at an angle of 90˚ to the disk for consistency. Each titanium disk received a single treatment procedure by consistently moving the nozzle from the center to the periphery in four circular motions. The amount of time per treatment procedure was set at 10 seconds. Following air-abrasive debridement, all titanium disks were rinsed with Phosphate Buffer Saline (PBS) to remove potential deposits of the powders. Then, three chemical agents, saline (NaCl 0.9%; Hikari®, Hikari Pharmaceutical CO., Ltd, Tokyo, Japan), alkaline electrolyzed water (AAEW 0.05%, pH 9.0; EPIOS CARE®, EPIOS Corp., Tokyo, Japan) and the diluted hydrogen peroxide with distilled deionized water (H_2O_2 3%; Wako Pure Chemical Industries, Ltd., Osaka, Japan) were used in the present study. NaCl was used as a negative control. These three chemical agents were regulated at 40˚C in the water bath. Those specimens which treated with air-flow were immersed into each three chemical regents for 60 seconds; i) NaCl (Air + NaCl), ii) AAEW (Air + AAEW), iii) H_2O_2 (Air + H_2O_2), respectively (described in Fig. 2). Non-contaminated and untreated titanium disks (As-polished) were served as control. All treatments were performed by the same trained operator. The titanium samples employed in this study were summarized in Figure 2.

4) Assessment of surface wettability and treatment time-dependent changes for water wettability (Study I)

Water wettability of the titanium surfaces was examined by measuring the

contact angle of 4 μl distilled water on the titanium disks using an automatic contact angle measuring device (Phoenix Alpha, Surface Electro Optics, Suwon, Korea). The titanium disks were prepared by immersed in distilled deionized water or 5% NaOCl solution for 15 minutes, 6 hours, 12 hours and 24 hours.

5) Collagen I adsorption assay (Study I)

To confirm adsorption of collagen I, samples were incubated with collagen I-FITC conjugate (Sigma-Aldrich, St. Louis, MO, USA) for 1 hour. After three washes with phosphate-buffered saline (PBS), samples were observed by confocal laser scanning microscopy operated by EZ-C1 system software (Confocal laser scanning microscopy, ECLIPSE TE-2000, Nikon, Tokyo, Japan). The adsorption of collagen I was evaluated by measuring the mean gray value of 5 randomly chosen images from three specimens of each groups as the fluorescence intensity using IMAGE-J software (NIH, Bethesda, ML, USA).

6) Analysis of surface chemical properties (Study I & II)

These surfaces chemical properties were examined by X-ray photoelectron spectroscopy (XPS; ESCA-850, Shimadzu Co. Ltd., Kyoto, Japan). Ti 2p, O 1s, C 1s and N 1s spectra were obtained using an XPS with Mg Kα radiation operated at a 7 kV accelerating voltage and 30 mA current under the vacuum of 1×10^{-6} Pa. Additionally, in study II, the amount of the hydroxyl groups and the relative concentration of carbon and nitrogen to titanium (C_C/C_{Ti} and C_N/C_{Ti}) were calculated from XPS data.

7) Evaluation of biofilm removal (Study II)

According to the instruction reported by Schwarz et al. (2009), the residual biofilm area (RB) was evaluated after each treatment. Erythrosine dye was used to stain the *S. gordonii* biofilm grown on each titanium surface. The digital images were taken using a CCD camera (Nikon DS-5M, Nikon, Tokyo, Japan) mounted on a microscope (Nikon AZ100, Nikon, Tokyo, Japan). Digital images were evaluated using an image analyzer (Image J, NIH, Bethesda, ML, USA). For each titanium disk and after each

treatment, mean stained RB areas were measured as a percentage of the scanned surface. Scanning electron microscopy (SEM; S-3500N, HITACHI Co. Ltd.) was used to observe the images of titanium surfaces before and after each treatment. Each group titanium disks were placed in 24-well plates, using one per well. The samples were washed twice with PBS and fixed in 2.5% glutaraldehyde buffered in PBS. Subsequently, they were washed 6 × 5 minutes with PBS, dehydrated in ethanol/water mixtures of 50, 70, and 80% for 5 minutes each, 90% for 10 minutes and 100% for 20 minutes. The samples were then critical-point dried with CO_2 and sputter-coated with gold. The samples were examined by SEM operated at an accelerating voltage of 15 kV.

2. Evaluation of initial cytocompatibility on the titanium surface

1) Human bone marrow mesenchymal stem cells (hBMSCs) culture (Study I & II)

hBMSCs (Poietics^{TM}, Lonza, Switzerland) were cultured on 10 cm tissue culture dishes (Falcon BD, Franklin Lakes, NJ, USA) using mesenchymal stem cell basal medium with mesenchymal stem cell growth supplements (MSCGM; Lonza) containing fetal bovine serum (FBS), L-glutamine, and GA-1000 (Gentamicin/Amphotericin-B). The cells were cultured at 37°C in humid 5% CO_2 in air.

2) Initial cell attachment on the titanium surfaces (Study I & II)

Cell attachment on each titanium disks was evaluated by counting the number of attached cells. Subsequent to surface treatment, the titanium disks were placed into a 24-well plate and seeded with a density of 6.0×10^4 cells/cm^2. After incubation for 4 hours, the titanium disks were rinsed with PBS to remove unattached cells. Adherent cells were then detached using 0.05% trypsin-0.53 mM EDTA-4 Na (Invitrogen, Ltd., Paisley, UK) at 37°C for 5 minutes. An equal volume of PBS was added. The cells were collected by centrifugation and re-suspended in fresh growth medium. The number of cells in the suspension was measured with a hemacytometer.

3) Initial attached cell density analysis (Study I & II)

SEM was used to observe the density of cells attached to the titanium surface.

The disks were placed in 24-well plates, using one per well. The hBMSCs were seeded at a density of 5,700 cells/cm^2 and incubated for 4 hours. After incubation, the samples were washed twice with PBS and fixed in 2.5% glutaraldehyde buffered in PBS. The subsequent methods follow the method described in *evaluation of biofilm removal*.

4) Immunofluorescent staining of actin cytoskeleton (Study I & II)

Confocal laser scanning microscopy was used to examine cell morphology and cytoskeletal arrangement in the hBMSCs seeded onto titanium surfaces. The disks were placed into a 24-well plate and seeded at a density of 5,700 cells/cm^2. After 4 hours of culture, the cells were stained using the fluorescent dye rhodamine phalloidin (Molecular probes, OR, USA), a mouse anti-vinculin monoclonal antibody (Abcam, Cambridge, MA, USA) and then by a FITC-conjugated anti-mouse secondary antibody (Abcam). The area, perimeter, Feret's diameter, and circularity of the cells were quantified using Image J software.

5) Treatment time-dependent changes for the number of initial cell attachment (Study I)

The number of initial cell attachment was evaluated by previously described method. The titanium disks were prepared by immersed in 5% NaOCl solution or distilled deionized water for 15 minutes, 6 hours, 12 hours and 24 hours.

3. Bactericidal effect and cytotoxicity of chemical agents used in Study II

1) Bactericidal effect for S. gordonii (Study II)

S. gordonii was transferred into TY liquid culture medium. Turbidity was calibrated by measuring the absorption at OD_{660}: 1.0 (1.0×10^8 CFU/mL). These cells were centrifuged and treated with 1 mL of NaCl, AAEW or H_2O_2 in an Eppendorf tube for 60 seconds at room temperature. The microbial cells were then washed, centrifuged, and suspended in PBS. After a 10-fold serial dilution, 100 μL of each microbial sample was inoculated on a TY agar plate and incubated for 3 days. The total number of microorganisms grown on the agar plate was counted and estimated as the colony forming unit.

2) Determination of cytotoxicity using trypan blue staining assay (Study II)

hBMSCs were plated in 96-well plate at a concentration of 2×10^4 cells/well and incubated for 24 hours before the experiment. The medium and unattached cells were removed, then 100 μl of NaCl, AAEW or H_2O_2 was added to the wells and the plates were incubated for 60 seconds. In the trypan blue staining assay, trypan blue (100 μL) was added to each well; unstained (viable) cells and stained (dead) cells were counted under a microscope using a hematocytometer. Cell viability (%) was determined by dividing the viable cell count by the total (viable + non-viable) cell count.

4. Statistical analysis (Study I & II)

Statistical differences were evaluated using analysis of variance (ANOVA) with Tukey's tests and paired *t*-test. *p* value <0.05, 0.001 were considered statistically significant.

Results

1. The effects of NaOCl and H_2O immersed treatment on the aged titanium surface (Study I)

1) Water Wettability of titanium surface

The water contact angle of the Untreated titanium was 59.4 ± 2.1˚, indicating that the surface was hydrophobic. With the water immersion treatment or NaOCl treatment, the contact angle substantially decreased (7.86 ± 2.9˚ and 3.81 ± 0.6˚ respectively), showing that the hydrophobic surface of these aged titanium was converted to the super hydrophilic surface ($\theta < 5^{\circ}$) (Fig. 3).

2) Collagen I adsorption capacity of titanium

Figure 4 shows the fluorescence intensity of collagen I-FITC conjugate attached on Untreated, H_2O-treated and NaOCl-treated disks. The fluorescence intensity of NaOCl was significantly higher than that of the other groups. In addition, the fluorescence intensity of H_2O-treated was significantly higher than that of Untreated.

3) Initial attached cell density

Figure 5A shows the relative number of cells attached to the titanium surfaces, as measured with the hemocytometer. The number of cells attached to the NaOCl-treated titanium and H_2O-treated titanium was twice greater than that to the Untreated titanium. There were no significantly different between NaOCl-treated titanium and H_2O-treated titanium. These results of Untreated, H_2O-treated and NaOCl-treated titanium surfaces were consistent with what could be observed under SEM in terms of cell density on these titanium surfaces examined (Fig. 5B).

4) Cell morphology and cytoskeletal arrangement of initial attached cells

Confocal laser scanning microscopic images of the hBMSCs after staining with rhodamine phalloidin showed that the cells after 4 hours of incubation on the NaOCl-treated titanium were clearly larger than on the Untreated and H_2O-treated titanium surfaces. Cells on the NaOCl-treated titanium surfaces were enlarged with a

clear stretch of lamellipodia-like actin projections and stressed fibers within their cytoplasm (Fig. 6A). Cytomorphometric evaluations for the area, perimeter and Feret's diameter of the cells showed greater values of these parameters on the NaOCl-treated titanium surface than on the Untreated titanium surfaces (Fig. 6B). In particular, the actin area of the cells on the NaOCl-treated titanium disk was significantly larger than that on the H_2O-treated and the Untreated titanium.

5) Evaluation of surface chemical properties

Figure 7 shows Ti 2p (A), C 1s (B), O 1s (C) and N 1s (D) spectra obtained from each titanium samples. The intensity of the Ti 2p peak at 454.0 eV which corresponds to the titanium in a metallic state was slightly lower for the H_2O-treated than the Untreated, suggesting that the thickness of surface oxide film increased during water immersion treatment (Fig. 7A). There was no significant change in the spectral intensity of the C 1s peak at 285.0 eV for aliphatic hydrocarbons between the H_2O-treated and the Untreated. The intensity of the C 1s peak at 288.0 eV attributed to carboxyl group or carbonyl group was slightly lower for the H_2O-treated than that for the Untreated (Fig. 7B). The N 1s peak at 400.0 eV was attributed to organic contaminants adsorbed on the titanium surface during the storage in dark place for two weeks. No noticeable change in the intensity of the N 1s peak was observed before and after water immersion treatment. Figure 8 shows that percent area of hydroxyl groups in O 1s spectra at before and after immersion in deionized water. Two types of hydroxyl groups: acidic hydroxyl group (a) and basic hydroxyl group (b) are present on the surface oxide film of titanium (Boehm, 1971). The percent area of the hydroxyl groups was increased by 3.8% for the acidic hydroxyl group and 0.5% for the basic hydroxyl group after water immersion treatment for 24 hours.

Figure 9 shows Ti 2p (A), C 1s (B), O 1s (C) and N 1s (D) spectra obtained from the Untreated and the NaOCl-treated. The intensity of the Ti 2p peak at 454.0 eV attributed to the titanium in a metallic state was much lower for the NaOCl-treated than that for the Untreated (Fig. 9A), suggesting that the thickness of the oxide film on the titanium disk increased during the NaOCl treatment. From the relative intensity for the peak at 454.0 eV with respect to the peak at 458.7 eV attributed to TiO_2 shown in Figures

7A and 9A, the thickness of the oxide film was greater for the NaOCl-treated than for H_2O-treated. Unlike water immersion treatment, intensity of the C 1s peak at 288.0 eV and the N 1s peak at 400.0 eV was substantially decreased after NaOCl treatment (Fig. 9B and D). Both the percent area of the hydroxyl groups was increased by 4.8% for the acidic hydroxyl group and 0.6% for the basic hydroxyl group after 5% NaOCl treatment (Fig.10), suggesting that the number of both hydroxyl groups on the oxide film was larger after NaOCl treatment than after water immersion treatment (Figs. 8 and 10).

6) Treatment time-dependent changes for water wettability and the number of initial cell attachment

Figure 11 shows water contact angle and the variation of a relative number of cells attached to the titanium surface with the treatment time. It was found that NaOCl treatment for 15 minutes is effective to convert to the hydrophilic surface, but it takes 12 hours for water immersion treatment to convert to the hydrophilic surface. Correspondingly, it was found that NaOCl treatment for 15 minutes is effective in increasing number of attached cells but it takes 6 hours for water immersion treatment.

2. The effects of chemical agents used following air-abrasive debridement on experimentally contaminated titanium surfaces with respects to changes of surface chemical properties and of initial cytocompatibility (Study II)

1) Cytotoxicity and bactericidal effect of titanium surface treatments

Cytotoxicity levels following AAEW and H_2O_2 treatments were significantly higher than that of NaCl treatment. There was no significant difference in cytotoxicity between AAEW and H_2O_2 treatments (Fig. 12A). The bactericidal effects following AAEW and H_2O_2 treatments were significantly higher than that of NaCl treatment. There was no significant difference in bactericidal effect between AAEW and H_2O_2 treatments (Fig. 12B).

2) Evaluation of biofilm removal

SEM analysis showed that all untreated titanium disks were completely and

homogeneously covered by an *S. gordonii* biofilm, as determined by erythrosine dye (Fig. 13A). Similarly, the entire disk surface of the biofilm contaminated titanium was colonized by a dense network of multiple layers of *S. gordonii* (Fig. 13B). All treatment groups resulted in complete and significant removal of the *S. gordonii* biofilm as determined by RB area (%) (Fig. 13C). Additionally, powder deposition was not observed on any of the treatment group surfaces.

3) Initial attached cell density

Numbers of initial cells attached to the Air + AAEW treated and As-polished surfaces were approximately 2-fold greater compared with the Air + NaCl treated surfaces. There was no significant difference in the number of attached cells between the Air + NaCl and Air + H_2O_2 treated surfaces (Fig. 14A). SEM images of cell density on the titanium surfaces confirmed these results (Fig. 14B). Cells failed to attach to the biofilm contaminated disks (data not shown).

4) Cell morphology and cytoskeletal arrangement of initial attached cells

Cytomorphometric evaluation of the actin area of the initial attached cells showed that cells on the Air + AAEW treated surfaces were significantly larger than those on the Air + NaCl and Air + H_2O_2 treated surfaces (Fig. 15A). Of note, cell area on the Air + AAEW treated surfaces was almost equal to that on the As-polished surfaces (Fig. 15A). There was no initial cell attachment to the biofilm contaminated disk (data not shown).

Confocal microscopy images clearly showed that the cells were larger on the Air + AAEW treated surfaces compared with on the Air + NaCl and Air + H_2O_2 treated surfaces. Cells on the Air + AAEW treated and As-polished surfaces were enlarged with clear lamellipodia-like actin projections (Fig. 15B).

5) Evaluation of surface chemical properties

Representative spectra of each treatment are shown in Figure 16. The results show that the biofilm contaminated titanium surface had a significantly increased

intensity of C 1s and N 1s, while the intensity of O 1s and Ti 2p were markedly decreased. This indicated that the organic compounds containing nitrogen (organic nitrogen deposits: ONDs), provided by the *S. gordonii* biofilm, completely covered the underlying titanium surfaces (Fig. 16). Considering all three treatment groups, the Air + AAEW treated surface most closely reflected that of the As-polished surface with respect to intensity at atomic level. The XPS data showed that after treatment, Air + NaCl, Air + AAEW and Air + H_2O_2 induced a significant decrease in the amounts of carbon and nitrogen on each titanium surface (Table 1). However, the C_N/C_{Ti} results demonstrated that nitrogen remained on the titanium surface after each treatment, except for on the Air + AAEW treated surface (Table 1). In fact, the C_N/C_{Ti} data for the Air + AAEW treated surface was comparable to that of the As-polished surface (Table 1). Moreover, the C_N/C_{Ti} data for the Air + AAEW treated surface was significantly reduced compared with that of Air + NaCl and Air + H_2O_2 treated surfaces ($p< 0.05$). There were no significant differences for C_C/C_{Ti} data among all sample groups, except for the biofilm-contaminated group.

Discussion

The current thesis of studies has investigated the surface decontamination procedures for volatile organic compounds (VOCs) contaminated titanium (study I) and bacterial biofilm contaminated titanium (study II) in vitro.

VOCs contamination is inevitably occurred before implant placement. Since Att et al. (2009) demonstrated that the phenomenon of biological aging was observed markedly within 2 weeks, the Untreated titanium disks were used as a specimen in this study. In discussion, the process for adsorption of VOCs to the pristine titanium surfaces and desorption of VOCs from the aged titanium surface with water immersion treatment and NaOCl treatment were discussed.

In the latter part of discussion, the chemical surface treatment with AAEW evaluated in study II was focused. To my knowledge, this is the first study reporting the effects of AAEW treatment of contaminated titanium surfaces, following air-abrasive debridement, for effectively removing biofilm and restoring an optimal surface for the initial attachment of hBMSCs. The surface chemical properties were evaluated to better understand differences in titanium surface cytocompatibility following various treatments. Mechanically-polished smooth titanium disks were utilized as a control to exclude the influence of surface roughness. Because *S. gordonii* is a known initial colonizer of the oral biofilm and is routinely identified in peri-implantitis patients, the titanium surfaces were experimentally-contaminated with a *S. gordonii* biofilm (Shibli et al., 2008; Koyanagi et al., 2013). This *in-vitro* data provided knowledge suggesting a potential cleaning method, which is beneficial for restoring surface cleanness and cytocompatibility.

1. Biological aging and chemical surface treatment (Study I)

1) *The process for adsorption of volatile organic compounds (VOCs) in air and its relation to biological aging of titanium*

The adsorption of VOCs in air on the titanium surface, which changes the hydrophilic titanium surface to hydrophobic, has considered to be responsible for this biological degradation of titanium. It has been also well known that these VOCs

adsorbed instantaneously on most solid substances including titanium. Consequently, when the surface was analyzed by X-ray photoelectron spectroscopy (XPS), strong C 1s peak was always observed at 284.5-285.0 eV as far as the samples was processed in air before leading them to the high vacuum chamber of XPS (Serro & Saramago, 2003; Att et al., 2009). There were similar observations in our results of XPS assay (Figs. 7 and 8). In contrast to this, biological aging of titanium reported in literature was rather a slow process. Most titanium surfaces immediately after processing in air showed superhydrophilic status ($\theta < 5^{\circ}$) (Aita et al., 2009; Att et al., 2009; Att & Ogawa, 2012; Minamikawa et al., 2016). These facts suggested that VOCs initially adsorbed on the titanium surface resulted in limited influences on the hydrophilicity and biological activities of titanium. Physical adsorption of VOCs on titanium surface is instantaneous and in the low pressure region of the adsorption isotherm where Henry's law is valid, the amount of VOCs is proportion to the partial pressure (or concentration) of each VOC in air;

$$X = K_H P \qquad (1)$$

where X is the surface coverage, P the partial pressure, and K_H the Henry's adsorption constant. Among VOCs in air, the average concentration of alkanes (aliphatic saturated hydrocarbons) such as methane, ethane and propane is about 2 ppm which is approximately three orders of magnitudes higher than other VOCs. It can easily be deduced from this fact that most adsorbed contaminants initially adsorbed on titanium surface would be these aliphatic saturated hydrocarbons. Physical adsorption of these hydrocarbons without polar groups is caused by van der Waals force, suggesting that these adsorbed hydrocarbons can be easily replaced by water molecules which interact with surface hydroxyl groups of titanium by hydrogen bond when water is dropped on the titanium surface to measure contact angle.

Att et al. (2009) showed that the initial hydrophilic surface of titanium gradually changed to hydrophobic and biological degradation of titanium progressed in time-dependent manner. In this study, it was also demonstrated that the water contact

angle of the Untreated titanium was about 60˚ (Fig. 3), indicating the surface was hydrophobic. These results suggested the presence of hydrophobic organic impurities which interacted with titanium surface stronger than aliphatic saturated hydrocarbons. The atmospheric gas phase contains a variety of VOCs with polar groups, such as amines, aldehydes, alcohols, carboxylic acids, etc. (Mellouki et al., 2015). Although the concentration of these molecules in the atmosphere is quite low, in the range from ppt to several ppb levels, they can interact with the surface hydroxide groups of titanium by hydrogen bond, as shown in Figure 17. With aging in air, the initially adsorbed saturated hydrocarbons were gradually removed from the titanium surface by replacing with these more preferentially adsorbed VOCs with polar groups and consequently, the hydrophilic titanium surface was changed to hydrophobic.

2) *Desorption of VOCs from the aged titanium surface with water immersion treatment.*

With water immersion treatment for 24 hours, the contact angle of water droplet significantly decreased from 59.4˚ to 7.9˚ (Fig. 3). In addition to VOCs physically adsorbed by van der Waals force, a large number of adsorbed VOCs by hydrogen bonds were probably subjected to hydrolysis and removed from the titanium surface as shown in Figure 7B. Significant decrease in C 1s peak at around 288.0 eV due to carboxyl or carbonyl groups shown in Figure 7B supported this assumption. This hydrolysis process, however, was so slow that the adsorbed VOCs with polar groups on the aged titanium surface were not removed during the water contact angle measurement unlike the adsorbed aliphatic saturated hydrocarbons. Water immersion treatment was thus useful for removing some VOCs with polar groups and increasing acidic hydroxyl groups but its effect is limited. There was no significant difference in spectral intensity of the N 1s peaks before and after the water immersion treatment, suggesting that few atmospheric organic-nitrogen compounds such as amines and amides were removed from the surface during the treatment. No significant change was also observed in the intensity of the main C 1s peak at 284.5 eV attributed to adsorbed saturated hydrocarbon between Untreated and H_2O-treated titanium. This is due to the instantaneous adsorption of saturated hydrocarbons on the titanium surface, which took place during the processing

of the titanium specimen in air before introducing it into high vacuum chamber of XPS. As already mentioned, this physical adsorption of saturated hydrocarbons is inevitable and very fast but these adsorbed hydrocarbons do not affect the hydrophilicity of titanium surface. Using some typical bond energy values (Kinloch, 1987; Allen et al., 1992; Lee, 1993) for hydrogen bonds (about 25 kJ/mol for O−H···O, 23 for O−H···N, 10 for N−H···O, 8 for C−H···O) and van der Waals force (less than 2 kJ/mol for the induced force), the replacement of VOCs from titanium surface can be discussed as follows. When a non-polar alkane type VOC is replaced by a water molecule (Fig. 17A), the system would be stabilized by as much as (−2) − (−25 × 2) = 48 kJ/mol. In case of the replacement of a VOC of amine type by a water (Fig. 17B), the stabilization energy amounts to [(−10) + (−23)] – (−25×2) = 17 kJ/mol. Similarly, for the aldehyde type VOC (Fig. 17C), the energy stabilization with the replacement by water may become [(−10) + (−25)] – (−25×2) = 15 kJ/mol. Although this is a semi-quantitative and a rough estimation, still it can explain why nonpolar VOCs (hydrocarbons) are more easily replaced by water than those with polar functional groups.

3) *Effects of sodium hypochlorite on removal of adsorbed VOCs with polar groups from the aged titanium surface*

5% Sodium hypochlorite is widely used as an oxidizing and a disinfectant (Mountouris et al., 2004; Mohammadi, 2008). This chlorine compound has been reported to react with a number of organic compounds including biological molecules at physiological pH conditions (Hawkins et al., 2003). With NaOCl treatment for 24 hours, the contact angle of water droplet significantly decreased from 59.4˚ to 3.8˚, which was much lower than that with water immersion treatment (Fig. 3). Moreover, NaOCl treatment for 15 minutes is effective to convert to the hydrophilic surface in a short time as compared with water immersion treatment (Fig. 11). The XPS spectral intensity both C 1s peak at 288 eV and N 1s peak at 400 eV due to VOCs with polar groups also decreased significantly with NaOCl treatment. Especially, organic nitrogen compounds which remained after water immersion treatment were obviously removed from the titanium surface by NaOCl treatment. Since ClO^- was reported to react readily with

amines, the adsorbed amines probably reacted with ClO^- to yield chloramines (reactions 2 and 3) and desorbed from the titanium surface as shown in Figure 17.

$$R-NH_2 + ClO^- \rightarrow R-NHCl + OH^- \quad (2)$$

$$R-NH_2 + 2ClO^- \rightarrow R-NCl_2 + 2OH^- \quad (3)$$

Amides can also react with NaOCl to yield chloramine (reaction 4) and they desorb from the titanium surface as well.

$$R-CONH_2 + ClO^- \rightarrow R-CONHCl + OH^- \quad (4)$$

Owing to these strong oxidation reaction, it was possible to decompose the VOCs with polar groups that could not be removed by water immersion treatment. In the previous section, it was discussed that VOCs could be replaced by water on the polar titanium surface, based on the energetic stabilization of the system. It was also indicated that the polar VOCs are more difficult to be removed than nonpolar VOCs in water. However, the equilibrium shifts toward the detachment if the detached VOCs are removed from the system, for example, by the oxidative decomposition. Due to this equilibrium displacement in the presence of ClO^-, even the polar VOCs could be removed from the titanium surface. Hence, the recovery of titanium wettability by ClO^- can be explained.

4) *Enhanced initial cytocompatibility of aged titanium surface with NaOCl treatment.*

Early studies already reported about the importance of chemically clean implant surfaces and the technique of radio frequency glow-discharge (RFGD) treatments to achieve decontaminated surfaces with high surface energy (DePalma et al., 1972). Baier et al. (1984) observed a strong influence of the initial surface state of cleanliness and surface free energy of an implant on the healing process and generation of host tissue cells adjacent to the implant surface.

In the present study, initial cell attachment and morphology were evaluated to

confirm early cell response to each titanium surface. After implantation, implant surfaces are in contacts with body fluids and interact with a number of proteins and different cell types. The initial cell behavior on the implant surface is the key factor in determining the osteoconductive capacity of implants during the early stage of osseointegration (Marinucci et al., 2006). The quantity and quality of cell attachment on titanium surfaces play a critical role in determining the subsequent process of osseointegration (Lee & Ogawa, 2012). The number of osteogenic cells attached to titanium may directly affect the volume of peri-implant bone formation (Lee & Ogawa, 2012). Enhanced cell spread and cytoskeletal formation at an initial stage of cell attachment to biomaterial surfaces ensure the retention and prompt onset of cellular function. Protein adsorption is also key biologic steps to initiate the cascade of bone-titanium integration (Hori et al., 2010). Figure 5 showed the number of initial cells attached to the NaOCl-treated titanium and H_2O-treated titanium was twice greater than that to the Untreated titanium surface. Interestingly, confocal laser scanning microscopic images of the hBMSCs after staining with rhodamine phalloidin showed that the cells after 4 hours of incubation on the NaOCl-treated titanium were clearly larger than those on the Untreated titanium and H_2O-treated titanium. Cells on the NaOCl-treated titanium surfaces were enlarged with a clear stretch of lamellipodia-like actin projections and stressed fibers within their cytoplasm (Fig. 6A). Cytomorphometric evaluations of the area, perimeter, and Feret's diameter of hBMSCs demonstrated that there was no significant difference of these parameters between H_2O-treated and Untreated, while greater values of these parameters on the NaOCl-treated titanium surface than on the Untreated titanium surfaces ($p< 0.05$; Fig. 6B). In particular, the actin area of the cells on the NaOCl-treated titanium was about 3 times larger than that on the Untreated titanium (Fig. 6B). Iwasa et al. (2010) has reported that the area of osteoblasts after staining with rhodamine phalloidin showed that the cells were about 3 times larger on UV-treated acid-etched titanium surfaces than on 4-week-old titanium acid-etched surfaces after 3 hours of incubation. This finding is comparable to the results of the present study. Taken together, it was suggested that the effects of NaOCl resulted in the enhanced cytocompatibility of titanium compared with Untreated or H_2O-treated titanium surface. There is one possibility that an increase in the

quantities of hydroxyl groups occurring on the NaOCl-treated titanium surface can be contributed to improve the cytocompatibility on the NaOCl-treated titanium surface. Feng et.al. (2003) had reported that the effect of the oxide films on initial adhesion of osteoblasts was investigated and the surface chemistry of substrate after the cell culture was evaluated by surface analyses. The authors concluded that the amounts of surface OH groups (basic OH groups and acidic OH groups), significantly influenced the initial behavior of the osteoblasts on the titanium surfaces. In addition, the present study demonstrated that collagen I adsorption on the NaOCl-treated titanium surface was more increased than on the H_2O-treated surfaces (Fig. 4). As a result, it is thought that the increase of the adherent cell area and the cell which enlarged with a clear stretch of lamellipodia-like actin projections and stressed fibers within their cytoplasm was observed.

2. Surface decontamination for the biofilm contaminated titanium disks (Study II)

1) *Do chemical agents required for removing the biofilm?*

All three treatments eliminated the biofilm structure from the titanium surfaces, indicating that mechanical debridement with air-flow was effective at removing the *S. gordonii* biofilm (Fig. 13). In this *in-vitro* design, chemical agents did not contribute to removing the biofilm. There is similar results were observed by Schwarz et al. (2009). The authors evaluated the influence of air-abrasive debridement on the removal of non-mineralized plaque biofilms, collected *in-vivo* on roughened titanium dental implant surfaces, using an intraoral splint system. The authors demonstrated that the biofilm were completely removed after treatment procedure with air flow and amino acid glycine powder (EMS) by consistently moving the nozzle from center to the periphery in four circular motions. This reports support our findings that air-abrasive debridement has a great potential removing the biofilm (Fig. 13).

2) *Do chemical agents contribute to restoring of cytocompatibility and surface chemical properties?*

In four *in-vitro* studies (Augthun et al., 1998; Schwarz et al., 2005; Schwarz et

al., 2009; John et al., 2014), decontamination procedures failed to restore biocompatibility of contaminated surfaces to the level of pristine controls. The reduced biocompatibility after mechanical treatment was attributed to changes in surface topography and chemical composition of the titanium oxide film produced by the instrumentation, but also to residual biofilm (Louropoulou et al., 2015). In fact, Mouhyi et al. (1998) evaluated the surface composition of failing and subsequently retrieved machined titanium implants after various cleaning procedures. Although some of the tested methods resulted in a macroscopically clean surface, all methods failed to re-establish the original surface elemental composition.

In the present study II, the number of attached cells and cell spreading were measured to evaluate the cytocompatibility on the treated titanium surfaces compared with pristine surface (As-polished). The data showed discrepancies for cell affinities among treatment groups, whereby: (1) the number of cells attached to the Air + AAEW treated surfaces was approximately 2-fold greater than that to the Air + NaCl treated surfaces; (2) cell spreading was enhanced on the Air + AAEW treated surfaces compared with the Air + NaCl or Air + H_2O_2 treated surfaces; (3) there was no significant different in the number of attached cells and cell spreading between the Air + AAEW and As-polished surfaces. These data indicates that chemical surface treatment with AAEW as an adjunctive to air-abrasive debridement could be effective for restoring of cytocompatibility to the level of the pristine surface. Within the limits of the present study, this new knowledge has a potential benefits for the resolution of the reduced biocompatibility after mechanical treatment. Several studies showed that surface treatment with NaCl following mechanical debridement may not be able to restore the previously contaminated surface to its original state (Persson et al., 2001; Schou et al., 2003; Schwarz et al., 2009). In addition, Persson et al. (2004) demonstrated in a preclinical study that surface treatment with H_2O_2 failed to reestablish osseointegration on surfaces at sites with experimentally induced peri-implantitis. These reports support our findings that the number of attached cells and overall cell area on the Air + NaCl and Air + H_2O_2 treated surface were significantly lower than those on the As-polished (Figs. 14 and 15). Although several factors might explain a lack of cell affinities following

NaCl or H_2O_2 treatment, the inferior properties of NaCl and H_2O_2 seems to be attributed to insufficient removal of ONDs observed by XPS evaluation. The C_N/C_{Ti} data for the Air + NaCl and Air + H_2O_2 was 0.0237 ± 0.0112 and 0.0210 ± 0.0054 respectively, which was significantly higher than that of the As-polished (0.0079 ± 0.0004) as shown in Table.1. This slightly remained ONDs may be possible to reduce the cytocompatibility. On the other hands, AAEW treatment significantly removed the ONDs to a greater extent than the other treatment, at atomic level (Fig. 16, Table 1). This superior property of Air + AAEW treatment in restoring the atomic characteristics of the titanium surface resulted in comparable hBMSC growth characteristics to the As-polished group (Figs. 14-16, Table 1). All these data, taken together with the results from the present study seem to indicate that the removal of biofilm alone may not be the crucial step in the treatment of peri-implantitis.

3) *The mechanism of action of AAEW solution for restoring the surface properties*

Mentioned previously the mechanism of the action of ClO^- described in "*Effects of sodium hypochlorite on removal of adsorbed VOCs with polar groups from the aged titanium surface"*, this theory could be also available to explain the mechanism in this section since AAEW contains 487.5 ppm of ClO^-. Although the ONDs observed in study II is totally different from the VOCs, ClO^- of AAEW have a potential to remove the ONDs as described in Figure 17B. It means that ONDs can also react with AAEW to yield chloramine (reaction 5) and they desorb from the titanium surface as well.

$$R-CONH_2 + ClO^- \rightarrow R-CONHCl + OH^- \quad (5)$$

Owing to these strong oxidation reaction, it was possible to decompose the ONDs with polar groups. ClO^- concentration is a major determining factor for the chlorine concentration required for the removal of protein (BSA) and acidic polysaccharide (pectin) from hard solid surfaces (Al_2O_3) (Urano & Fukuzaki, 2005). This reports indicate that a large number of proteins within ONDs might be decomposed by the action of AAEW, as investigated in this study.

Conclusions

1. NaOCl-mediated biofunctionalization of titanium surface contributes to a decrease in the intensity of the C 1s peak at 288 eV and N 1s peak and an increase in the surface hydroxyl groups, coincident with maturing of surface oxide film. The biofunctionalization of titanium surface was attributed by the OCl^- which has strong oxidation effect and has a potential to decompose the VOCs with polar groups. Consequently, NaOCl treatment of titanium surface markedly enhanced the adsorption of collagen I and the initial behavior of hBMSCs.

2. The study II indicates that following chemical surface treatment with the use of AAEW as an adjunctive to air abrasive debridement, a treatment that does not possess marked cytotoxicity, showed superior capacity in restoring titanium surface chemical properties compared with H_2O_2, resulting in comparable cytocompatibility towards hBMSCs to the As-polished titanium surface. However, further studies are needed to evaluate the effects of AAEW treatment on surfaces with varying degrees of roughness. Finally, preclinical and clinical studies are mandatory to determine the *in-vivo* effects of Air + AAEW surface treatment before this technique can be used in the clinic.

Acknowledgement

My research has started since I was a dental student in 2010. The lecture of Prof. Endo and the instruction of Assoc. Prof. Kado and Prof. Aita inspired me to do a research related with biomaterial, in particular implant surface. From this point, nothing would be happened if they did not give me the chance to start my research. I would like to express my deeply gratitude to them.

My research would have been a short period if I had not meet Prof. Furuichi. It was 2012 that I met him for the first time. His lecture was also inspired me regarding the importance of evidences from many literatures in the field of Periodontology, which attracted me to be a specialist of periodontology. After graduate, he gave me the opportunity to work with him as a Ph-D student and he gave me knowledge and skills in clinical periodontology. I am very honorable that I have had his mentorship.

I would like to express my gratitude to all staff in Department of Periodontology at Göteborg University, especially to Prof. Tord Berglundh. He accepted me to do a research for 1 year at his laboratory as an exchange Ph-D student. He introduced me into the forefront of science in the field of Periodontology and Implant dentistry and gave me valuable knowledges.

This work in study I was supported by GC, corp.. This study was supported in part by a Grant-in-Aid for Scientific Research (C) (22592191) from the Japan Society for the Promotion of Science. I appreciate their supports.

Finally, I would like to express my special thanks for all staff of Department of Periodontology and Endodontology at Health Sciences University of Hokkaido.

References

Aita H, Hori N, Takeuchi M, Suzuki T, Yamada M, Anpo M & Ogawa T. The effect of ultraviolet functionalization of titanium on integration with bone. Biomaterials 30: 1015-1025, 2009.

Al-Hashedi AA, Laurenti M, Benhamou V & Tamimi F. Decontamination of titanium implants using physical methods. Clinical oral implants research 28: 1013-1021, 2017.

Albrektsson T, Brånemark P-I, Hansson H-A & Lindström J. Osseointegrated titanium implants: requirements for ensuring a long-lasting, direct bone-to-implant anchorage in man. Acta Orthopaedica Scandinavica 52: 155-170, 1981.

Albrektsson T, Dahlin C, Jemt T, Sennerby L, Turri A & Wennerberg A. Is marginal bone loss around oral implants the result of a provoked foreign body reaction? Clinical implant dentistry and related research 16: 155-165, 2014.

Albrektsson T, Chrcanovic B, Jacobsson M & Wennerberg A. Osseointegration of Implants: A Biological and Clinical Overview. 2017.

Allen K, Walker M, Leonard RG, Brennan M, Quigley K, Heatley D & Watts JF Adhesion and adhesives: the analytical challenge. Analytical proceedings1992: Royal Society of Chemistry.

Att W, Hori N, Takeuchi M, Ouyang J, Yang Y, Anpo M & Ogawa T. Time-dependent degradation of titanium osteoconductivity: an implication of biological aging of implant materials. Biomaterials 30: 5352-5363, 2009.

Att W & Ogawa T. Biological Aging of Implant Surfaces and Their Restoration with Ultraviolet Light Treatment: A Novel Understanding of Osseointegration. International Journal of Oral & Maxillofacial Implants 27: 753-761, 2012.

Augthun M, Tinschert J & Huber A. In vitro studies on the effect of cleaning methods on different implant surfaces. Journal of periodontology 69: 857-864, 1998.

Baier R, Meyer A, Natiella J, Natiella R & Carter J. Surface properties determine bioadhesive outcomes: methods and results. Journal of biomedical materials research 18: 337-355, 1984.

Berglundh T, Armitage G, Araujo MG, Avila-Ortiz G, Blanco J, Camargo PM, Chen S, Cochran D, Derks J, Figuero E, Hammerle CHF, Heitz-Mayfield LJA, Huynh-Ba G, Iacono V, Koo KT, Lambert F, McCauley L, Quirynen M, Renvert S, Salvi GE, Schwarz F, Tarnow D, Tomasi C, Wang HL & Zitzmann N. Peri-implant diseases and conditions: Consensus report of workgroup 4 of the 2017 World Workshop on the Classification of Periodontal and Peri-Implant Diseases and Conditions. J Clin Periodontol 45 Suppl 20: S286-S291, 2018.

Boehm H. Acidic and basic properties of hydroxylated metal oxide surfaces. Discussions of the Faraday Society 52: 264-275, 1971.

Brånemark P. Osseointegrated implants in the treatment of the edentulous jaw. Scand J Plast Reconstr Surg 11, 1977.

Claffey N, Clarke E, Polyzois I & Renvert S. Surgical treatment of peri-implantitis. J Clin Periodontol 35: 316-332, 2008.

DePalma V, Baier R, Ford J, Gott V & Furuse A. Investigation of three-surface properties

of several metals and their relation to blood compatibility. Journal of biomedical materials research 6: 37-75, 1972.

Derks J & Tomasi C. Peri-implant health and disease. A systematic review of current epidemiology. J Clin Periodontol 42 Suppl 16: S158-171, 2015.

Duske K, Koban I, Kindel E, Schröder K, Nebe B, Holtfreter B, Jablonowski L, Weltmann KD & Kocher T. Atmospheric plasma enhances wettability and cell spreading on dental implant metals. Journal of clinical periodontology 39: 400-407, 2012.

E Jung R, Zembic A, Pjetursson BE, Zwahlen M & S Thoma D. Systematic review of the survival rate and the incidence of biological, technical, and aesthetic complications of single crowns on implants reported in longitudinal studies with a mean follow-up of 5 years. Clinical oral implants research 23: 2-21, 2012.

Feng B, Weng J, Yang B, Qu S & Zhang X. Characterization of surface oxide films on titanium and adhesion of osteoblast. Biomaterials 24: 4663-4670, 2003.

Hawkins C, Pattison D & Davies MJ. Hypochlorite-induced oxidation of amino acids, peptides and proteins. Amino acids 25: 259-274, 2003.

Hori N, Ueno T, Suzuki T, Yamada M, Att W, Okada S, Ohno A, Aita H, Kimoto K & Ogawa T. Ultraviolet light treatment for the restoration of age-related degradation of titanium bioactivity. Int J Oral Maxillofac Implants 25: 49-62, 2010.

Huang YR, Hung YC, Hsu SY, Huang YW & Hwang DF. Application of electrolyzed water in the food industry. Food Control 19: 329-345, 2008.

Ichioka, Y., Kado, T., Aita, H., Nezu, T., Furuichi, Y., & Endo, K. (2021). In vitro evaluation of NaOCl-mediated functionalization of biologically aged titanium

surfaces. Dental materials journal, 40(1), 74–83. https://doi.org/10.4012/dmj.2019-358;

Ichioka, Y., Kado, T., Mashima, I., Nakazawa, F., Endo, K., & Furuichi, Y. (2020). Effects of chemical treatment as an adjunctive of air-abrasive debridement on restoring the surface chemical properties and cytocompatibility of experimentally contaminated titanium surfaces. Journal of biomedical materials research. Part B, Applied biomaterials, 108(1), 183–191. https://doi.org/10.1002/jbm.b.34377.

Iwasa F, Hori N, Ueno T, Minamikawa H, Yamada M & Ogawa T. Enhancement of osteoblast adhesion to UV-photofunctionalized titanium via an electrostatic mechanism. Biomaterials 31: 2717-2727, 2010.

Jepsen S, Berglundh T, Genco R, Aass AM, Demirel K, Derks J, Figuero E, Giovannoli JL, Goldstein M, Lambert F, Ortiz-Vigon A, Polyzois I, Salvi GE, Schwarz F, Serino G, Tomasi C & Zitzmann NU. Primary prevention of peri-implantitis: managing peri-implant mucositis. J Clin Periodontol 42 Suppl 16: S152-157, 2015.

John G, Becker J & Schwarz F. Rotating titanium brush for plaque removal from rough titanium surfaces--an in vitro study. Clin Oral Implants Res 25: 838-842, 2014.

Kilpadi DV, Lemons JE, Liu J, Raikar GN, Weimer JJ & Vohra Y. Cleaning and heat-treatment effects on unalloyed titanium implant surfaces. International Journal of Oral & Maxillofacial Implants 15, 2000.

Kinloch A. Adhesion and Adhesives Chapman and Hall. New York, 1987.

Kono M, Aita H, Ichioka Y, Kado T, Endo K & Koshino H. NaOCl-mediated biofunctionalization enhances bone-titanium integration. Dent Mater J 34: 537-544, 2015.

Koyanagi T, Sakamoto M, Takeuchi Y, Maruyama N, Ohkuma M & Izumi Y. Comprehensive microbiological findings in peri-implantitis and periodontitis. J Clin Periodontol 40: 218-226, 2013.

Lee JH & Ogawa T. The biological aging of titanium implants. Implant Dent 21: 415-421, 2012.

Lee L-H. Roles of molecular interactions in adhesion, adsorption, contact angle and wettability. Journal of adhesion science and technology 7: 583-634, 1993.

Louropoulou A, Slot DE & Van der Weijden F. Influence of mechanical instruments on the biocompatibility of titanium dental implants surfaces: a systematic review. Clinical oral implants research 26: 841-850, 2015.

Marinucci L, Balloni S, Becchetti E, Belcastro S, Guerra M, Calvitti M, Lull C, Calvi EM & Locci P. Effect of titanium surface roughness on human osteoblast proliferation and gene expression in vitro. International Journal of Oral & Maxillofacial Implants 21, 2006.

Mellouki A, Wallington T & Chen J. Atmospheric chemistry of oxygenated volatile organic compounds: impacts on air quality and climate. Chemical reviews 115: 3984-4014, 2015.

Minamikawa H, Att W, Ikeda T, Hirota M & Ogawa T. Long-term progressive degradation of the biological capability of titanium. Materials 9: 102, 2016.

Mohammadi Z. Sodium hypochlorite in endodontics: an update review. International dental journal 58: 329-341, 2008.

Mouhyi J, Sennerby L, Pireaux JJ, Dourov N, Nammour S & Van Reck J. An XPS and

SEM evaluation of six chemical and physical techniques for cleaning of contaminated titanium implants. Clin Oral Implants Res 9: 185-194, 1998.

Mountouris G, Silikas N & Eliades G. Effect of sodium hypochlorite treatment on the molecular composition and morphology of human coronal dentin. Journal of Adhesive Dentistry 6, 2004.

Nishiguchi S, Kato H, Fujita H, Kim HM, Miyaji F, Kokubo T & Nakamura T. Enhancement of bone-bonding strengths of titanium alloy implants by alkali and heat treatments. Journal of Biomedical Materials Research Part A 48: 689-696, 1999.

Ogawa T & Nishimura I. Different bone integration profiles of turned and acid-etched implants associated with modulated expression of extracellular matrix genes. International Journal of Oral & Maxillofacial Implants 18, 2003.

Ozawa S, Ogawa T, Iida K, Sukotjo C, Hasegawa H, Nishimura R & Nishimura I. Ovariectomy hinders the early stage of bone-implant integration: histomorphometric, biomechanical, and molecular analyses. Bone 30: 137-143, 2002.

Parlar A, Bosshardt DD, Cetiner D, Schafroth D, Unsal B, Haytac C & Lang NP. Effects of decontamination and implant surface characteristics on re-osseointegration following treatment of peri-implantitis. Clin Oral Implants Res 20: 391-399, 2009.

Persson LG, Ericsson I, Berglundh T & Lindhe J. Osseintegration following treatment of peri-implantitis and replacement of implant components. An experimental study in the dog. J Clin Periodontol 28: 258-263, 2001.

Persson LG, Mouhyi J, Berglundh T, Sennerby L & Lindhe J. Carbon dioxide laser and hydrogen peroxide conditioning in the treatment of periimplantitis: an experimental study in the dog. Clin Implant Dent Relat Res 6: 230-238, 2004.

Pjetursson BE, Thoma D, Jung R, Zwahlen M & Zembic A. A systematic review of the survival and complication rates of implant-supported fixed dental prostheses (FDPs) after a mean observation period of at least 5 years. Clinical oral implants research 23: 22-38, 2012.

Renvert S, Polyzois I & Maguire R. Re-osseointegration on previously contaminated surfaces: a systematic review. Clin Oral Implants Res 20 Suppl 4: 216-227, 2009.

Renvert S & Polyzois I. Risk indicators for peri-implant mucositis: a systematic literature review. Journal of clinical periodontology 42, 2015.

Schou S, Holmstrup P, Jorgensen T, Skovgaard LT, Stoltze K, Hjorting-Hansen E & Wenzel A. Implant surface preparation in the surgical treatment of experimental peri-implantitis with autogenous bone graft and ePTFE membrane in cynomolgus monkeys. Clin Oral Implants Res 14: 412-422, 2003.

Schwarz F, Sculean A, Romanos G, Herten M, Horn N, Scherbaum W & Becker J. Influence of different treatment approaches on the removal of early plaque biofilms and the viability of SAOS2 osteoblasts grown on titanium implants. Clin Oral Investig 9: 111-117, 2005.

Schwarz F, Ferrari D, Popovski K, Hartig B & Becker J. Influence of different air-abrasive powders on cell viability at biologically contaminated titanium dental implants surfaces. Journal of Biomedical Materials Research Part B: Applied Biomaterials 88: 83-91, 2009.

Schwarz F, Mihatovic I, Golubovic V, Eick S, Iglhaut T & Becker J. Experimental peri-implant mucositis at different implant surfaces. Journal of clinical periodontology 41: 513-520, 2014.

Serro A & Saramago B. Influence of sterilization on the mineralization of titanium implants induced by incubation in various biological model fluids. Biomaterials 24: 4749-4760, 2003.

Shibli JA, Melo L, Ferrari DS, Figueiredo LC, Faveri M & Feres M. Composition of supra- and subgingival biofilm of subjects with healthy and diseased implants. Clin Oral Implants Res 19: 975-982, 2008.

Suzuki T, Hori N, Att W, Kubo K, Iwasa F, Ueno T, Maeda H & Ogawa T. Ultraviolet treatment overcomes time-related degrading bioactivity of titanium. Tissue Engineering Part A 15: 3679-3688, 2009.

Ueno T, Yamada M, Hori N, Suzuki T & Ogawa T. Effect of ultraviolet photoactivation of titanium on osseointegration in a rat model. International Journal of Oral & Maxillofacial Implants 25, 2010a.

Ueno T, Yamada M, Suzuki T, Minamikawa H, Sato N, Hori N, Takeuchi K, Hattori M & Ogawa T. Enhancement of bone–titanium integration profile with UV-photofunctionalized titanium in a gap healing model. Biomaterials 31: 1546-1557, 2010b.

Ueno T, Takeuchi M, Hori N, Iwasa F, Minamikawa H, Igarashi Y, Anpo M & Ogawa T. Gamma ray treatment enhances bioactivity and osseointegration capability of titanium. Journal of Biomedical Materials Research Part B: Applied Biomaterials 100: 2279-2287, 2012.

Urano H & Fukuzaki S. The mode of action of sodium hypochlorite in the cleaning process. Biocontrol Science 10: 21-29, 2005.

Weinlaender M, Kenney EB, Lekovic V, Beumer III J, Moy PK & Lewis S. Histomorphometry of bone apposition around three types of endosseous dental implants. International Journal of Oral & Maxillofacial Implants 7, 1992.

Yamamura K, Miura T, Kou I, Muramatsu T, Furusawa M & Yoshinari M. Influence of various superhydrophilic treatments of titanium on the initial attachment, proliferation, and differentiation of osteoblast-like cells. Dental materials journal 34: 120-127, 2015.

Yoshinari M, Matsuzaka K, Inoue T, Oda Y & Shimon M. Bio-functionalization of titanium surfaces for dental implants. Materials Transactions 43: 2494-2501, 2002.

Yoshinari M, Matsuzaka K & Inoue T. Surface modification by cold-plasma technique for dental implants—Bio-functionalization with binding pharmaceuticals. Japanese Dental Science Review 47: 89-101, 2011.

Table and Figures

Table 1. Relative concentration of carbon and nitrogen to titanium (C_C/C_{Ti} and C_N/C_{Ti}).

	C_C / C_{Ti} (mass%)	C_N / C_{Ti} (mass%)
As-polished	0.506 (±0.189) †	0.0079 (±0.0004) †
Biofilm-contamincated	3.142 (±1.183) §	0.6476 (±0.1824) §
Air + NaCl	0.328 (±0.023) †	0.0237 (±0.0112) ‡
Air + AAEW	0.307 (±0.100) †	0.0071 (±0.0020) †
Air + H_2O_2	0.338 (±0.083) †	0.0210 (±0.0054) ‡

C_C/C_{Ti} and C_N/C_{Ti} were calculated from XPS data. Data shown are the mean ± SD (n = 4); measurement values with the same letter revealed no statistically significant differences ($p < 0.05$ for significance). This table was published in Ichioka et al. (2020) and reused with permission from the journal.

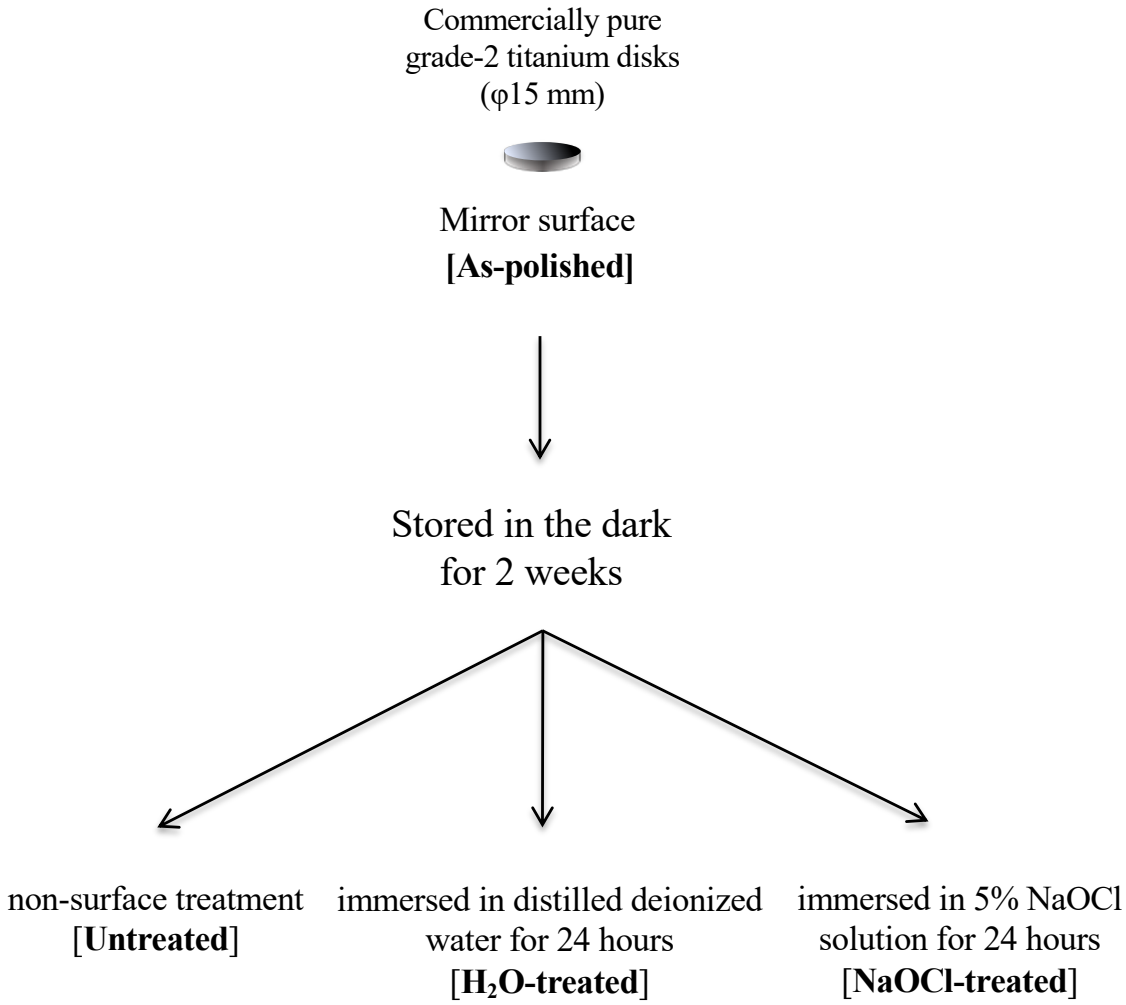

Figure. 1 Chemical surface treatments employed in study I. This figure was modified from the original figure published in Ichioka et al. (2021), Copyright 2021 The Japanese Society for Dental Materials and Devices, and reused with permission from the journal.

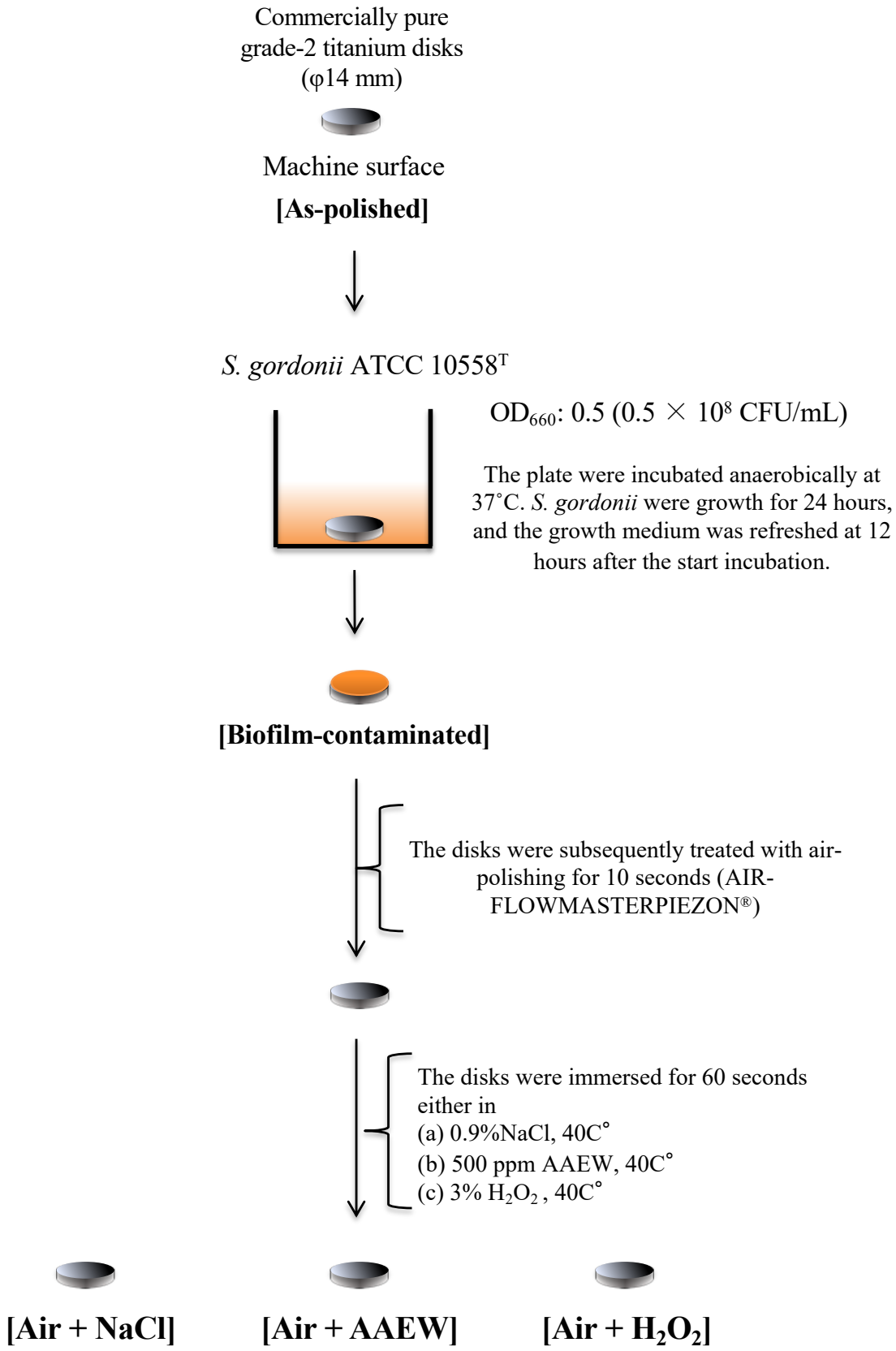

Figure. 2 Mechanical and chemical surface treatments employed in study II.

A

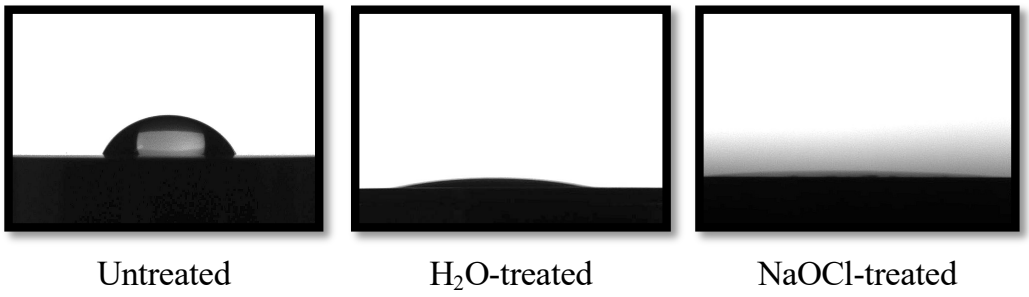

B

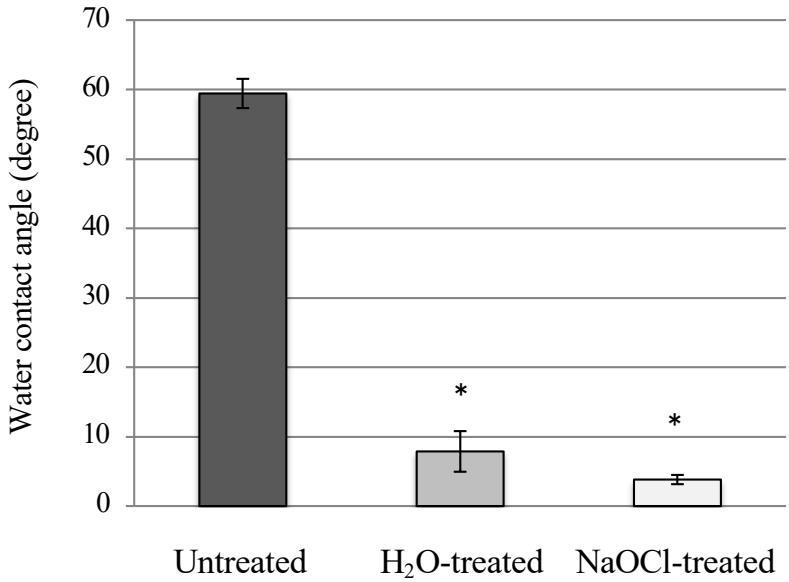

Figure. 3 (A) The image of 4 μl water droplets on the each titanium surface. (B) The water contact angle was obtained from image analysis of the 4 μl water droplets. Date are shown as mean ± SD (n = 5). *Indicate significant difference in comparison with Untreated ($p< 0.05$). This figure was published in Ichioka et al. (2021), Copyright 2021 The Japanese Society for Dental Materials and Devices, and reused with permission from the journal.

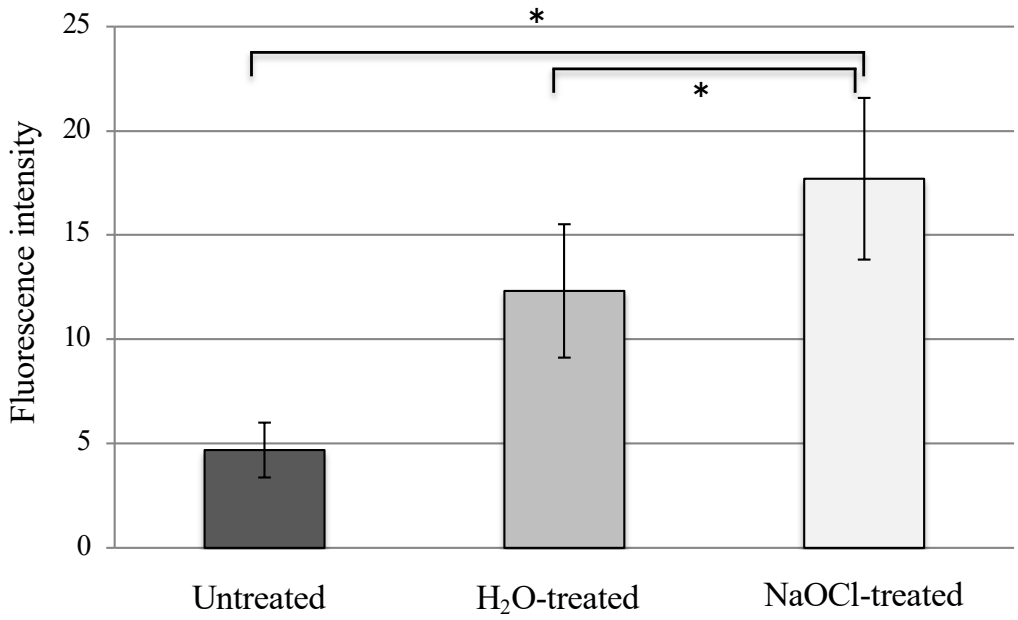

Figure. 4 The amount of adsorbed Collagen I on the each titanium surfaces. Fluorescence intensity was obtained by measuring the mean gray value of CLSM images using IMAGE-J software. Data are shown as the mean ± SD (n = 3). *: $p<$ 0.05 for significance. This figure was published in Ichioka et al. (2021), Copyright 2021 The Japanese Society for Dental Materials and Devices, and reused with permission from the journal.

A

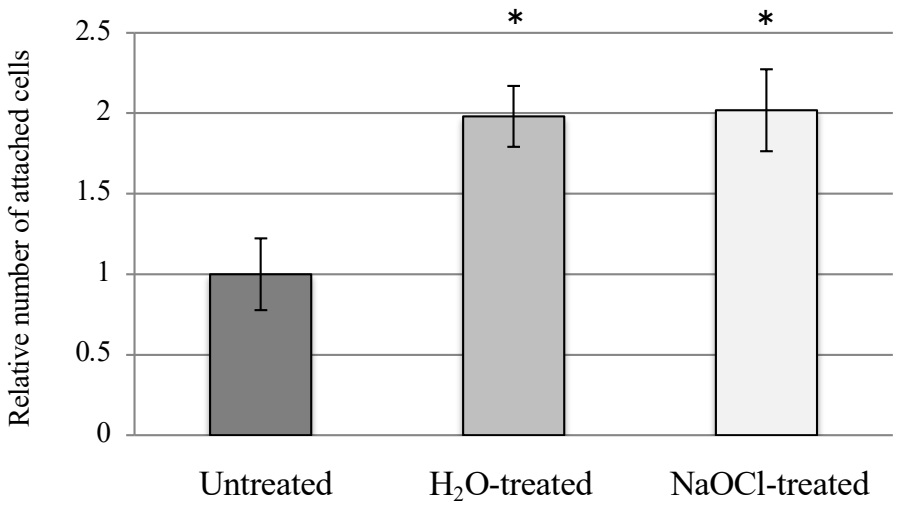

B

Figure. 5 (A) The relative number of attached hBMSCs 4 hours after seeding on the titanium surfaces measured with a hemocytometer. Data are shown as the mean ± SD (n = 4). *Indicate significant difference in comparison with Untreated ($p< 0.05$). (B) Cell density image (magnification x40) on the titanium surfaces as observed by SEM. This figure was published in Ichioka et al. (2021), Copyright 2021 The Japanese Society for Dental Materials and Devices, and reused with permission from the journal.

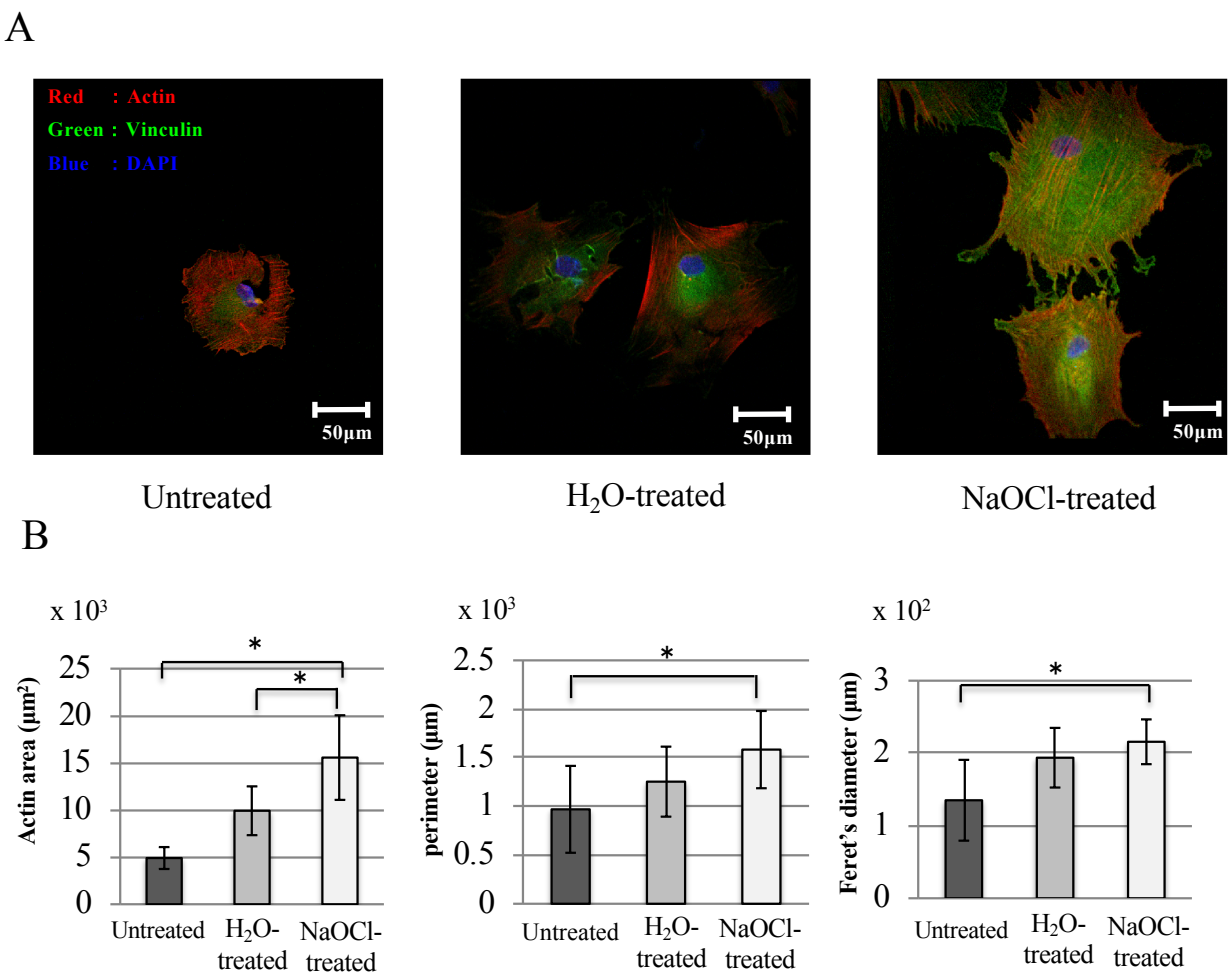

Figure. 6 (A) Fluorescent images of the hBMSCs on the titanium disks. (B) Cytomorphometric evaluations for the area, Perimeter and Feret's diameter of the cells. Data are shown as the mean ± SD (n = 5). *: $p < 0.05$ for significance. This figure was published in Ichioka et al. (2021), Copyright 2021 The Japanese Society for Dental Materials and Devices, and reused with permission from the journal.

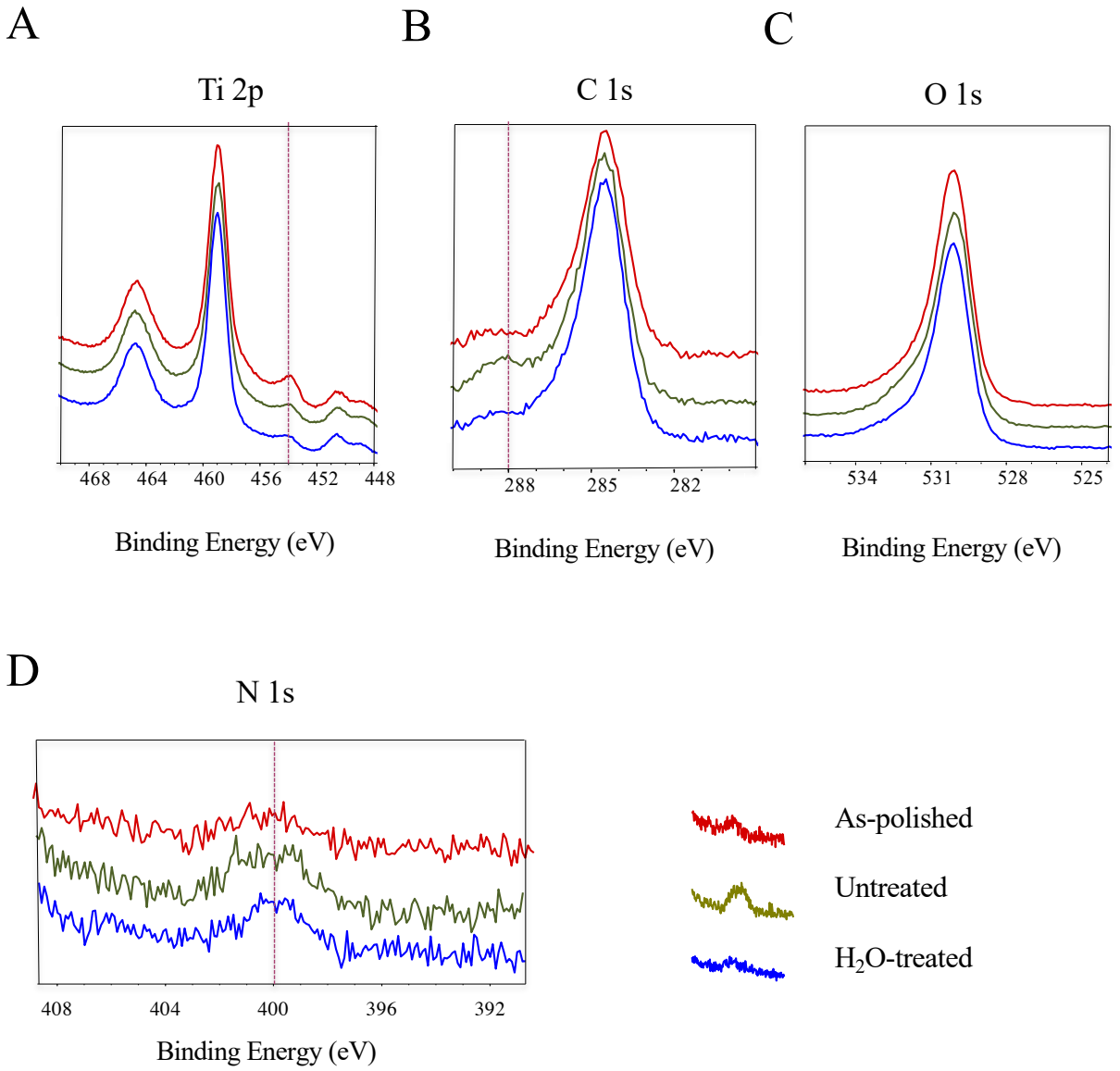

Figure. 7 Ti 2p, C 1s and N 1s spectra obtained from the same specimens at before and after immersion in deionized water. This figure was published in Ichioka et al. (2021), Copyright 2021 The Japanese Society for Dental Materials and Devices, and reused with permission from the journal.

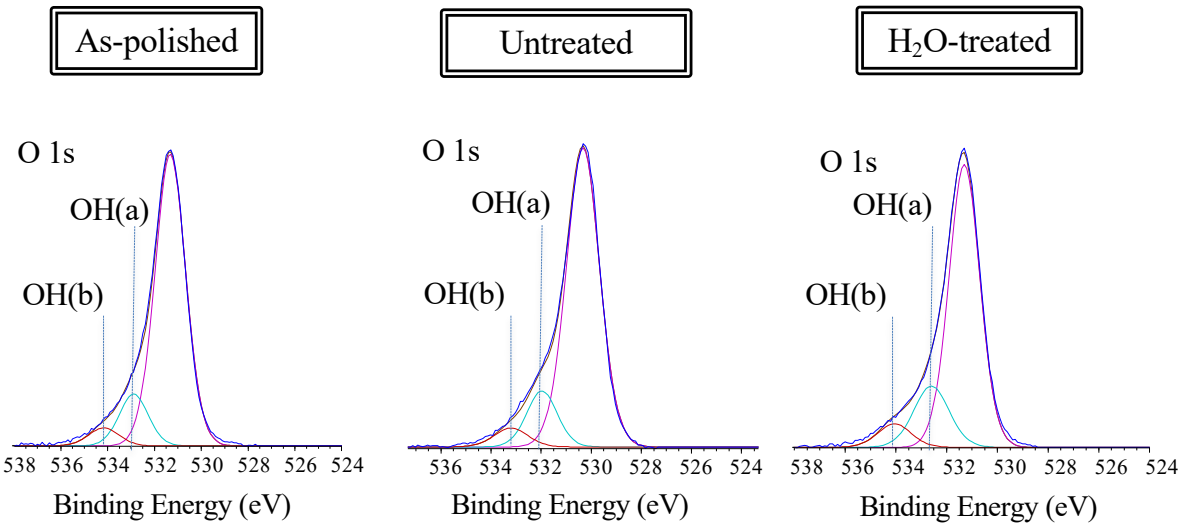

<<Percent area in O1s spectra>>

Name	OH(a)	OH(b)
As-polished	13.76%	5.05%
Untreated	13.87%	5.18%
H_2O-treated	**17.67%**	**5.68%**

Figure. 8 Percent area of hydroxyl groups in O 1s spectra at before and after immersion in deionized water. This figure was published in Ichioka et al. (2021), Copyright 2021 The Japanese Society for Dental Materials and Devices, and reused with permission from the journal.

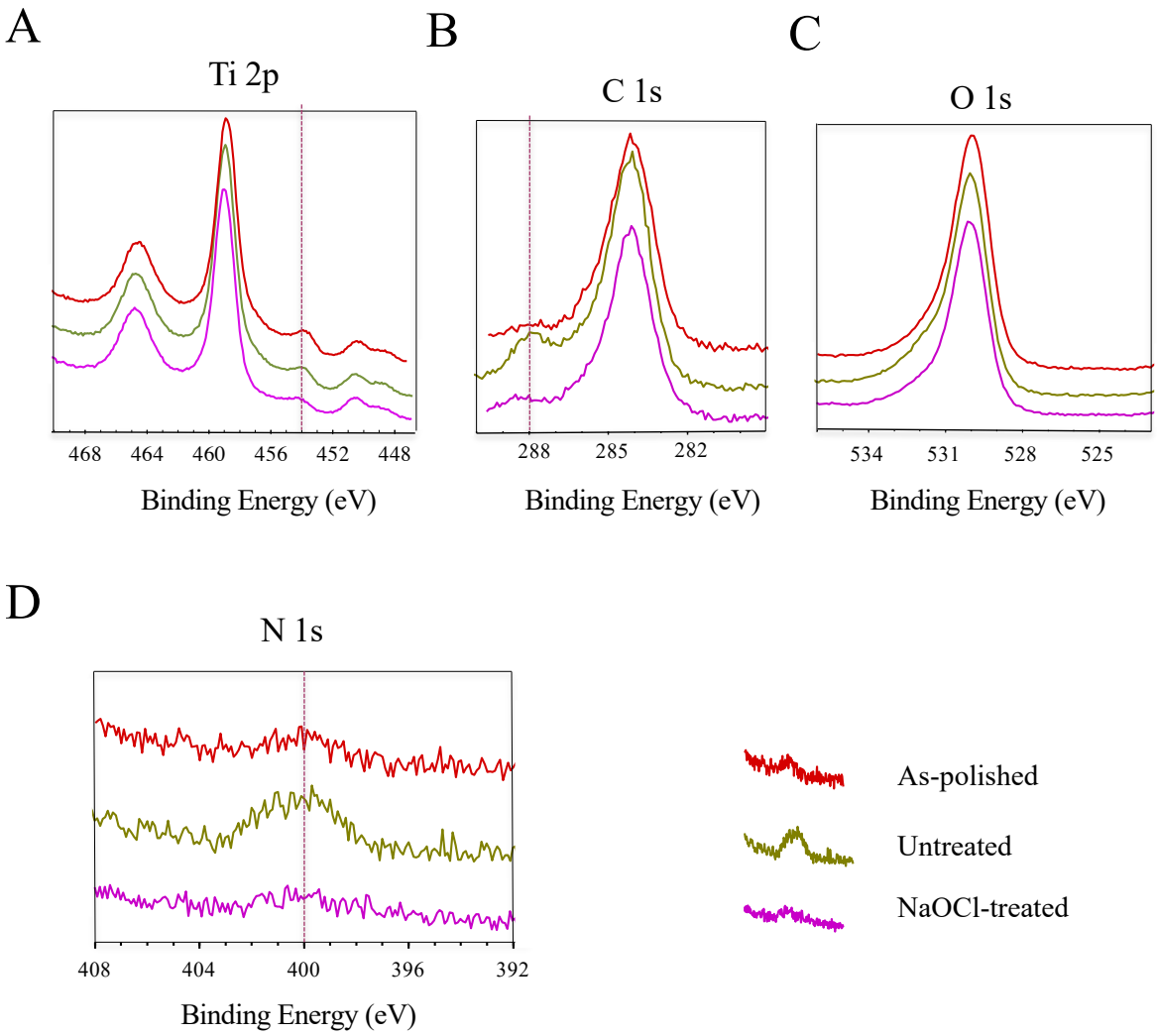

Figure. 9 Ti 2p, C 1s and N 1s spectra obtained from the same specimens at before and after immersion in NaOCl solution. This figure was published in Ichioka et al. (2021), Copyright 2021 The Japanese Society for Dental Materials and Devices, and reused with permission from the journal.

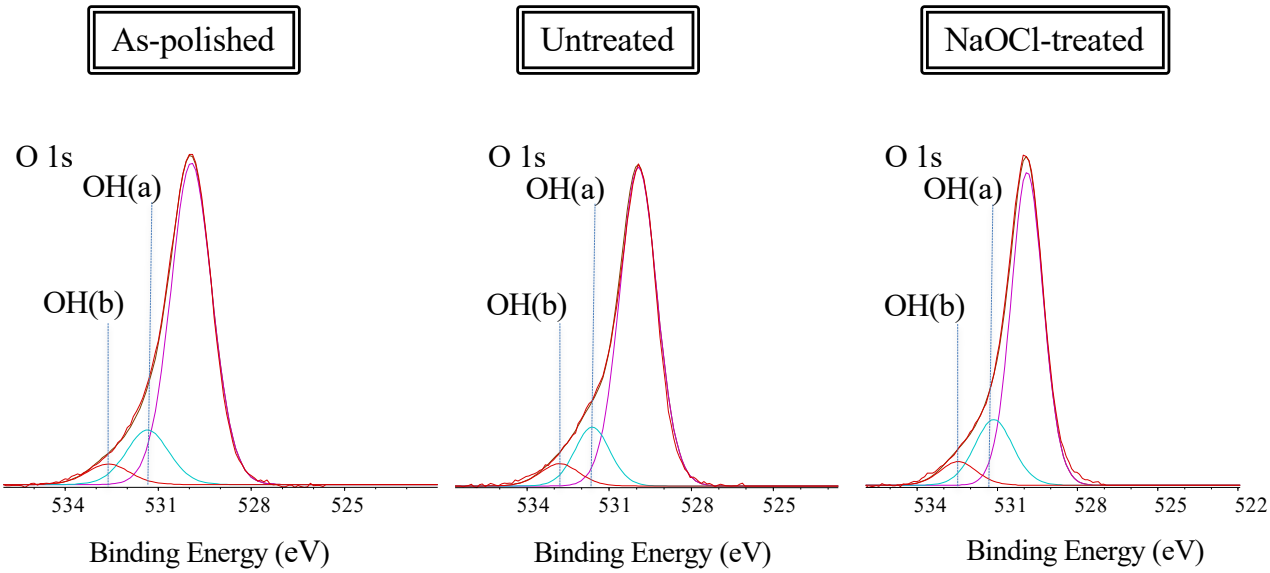

<<Percent area in O1s spectra>>

Name	OH(a)	OH(b)
As-polished	14.14%	5.28%
Untreated	13.93%	5.85%
NaOCl-treated	**18.72%**	**6.47%**

Figure. 10 Percent area of hydroxyl groups in O 1s spectra at before and after immersion in NaOCl solution. This figure was published in Ichioka et al. (2021), Copyright 2021 The Japanese Society for Dental Materials and Devices, and reused with permission from the journal.

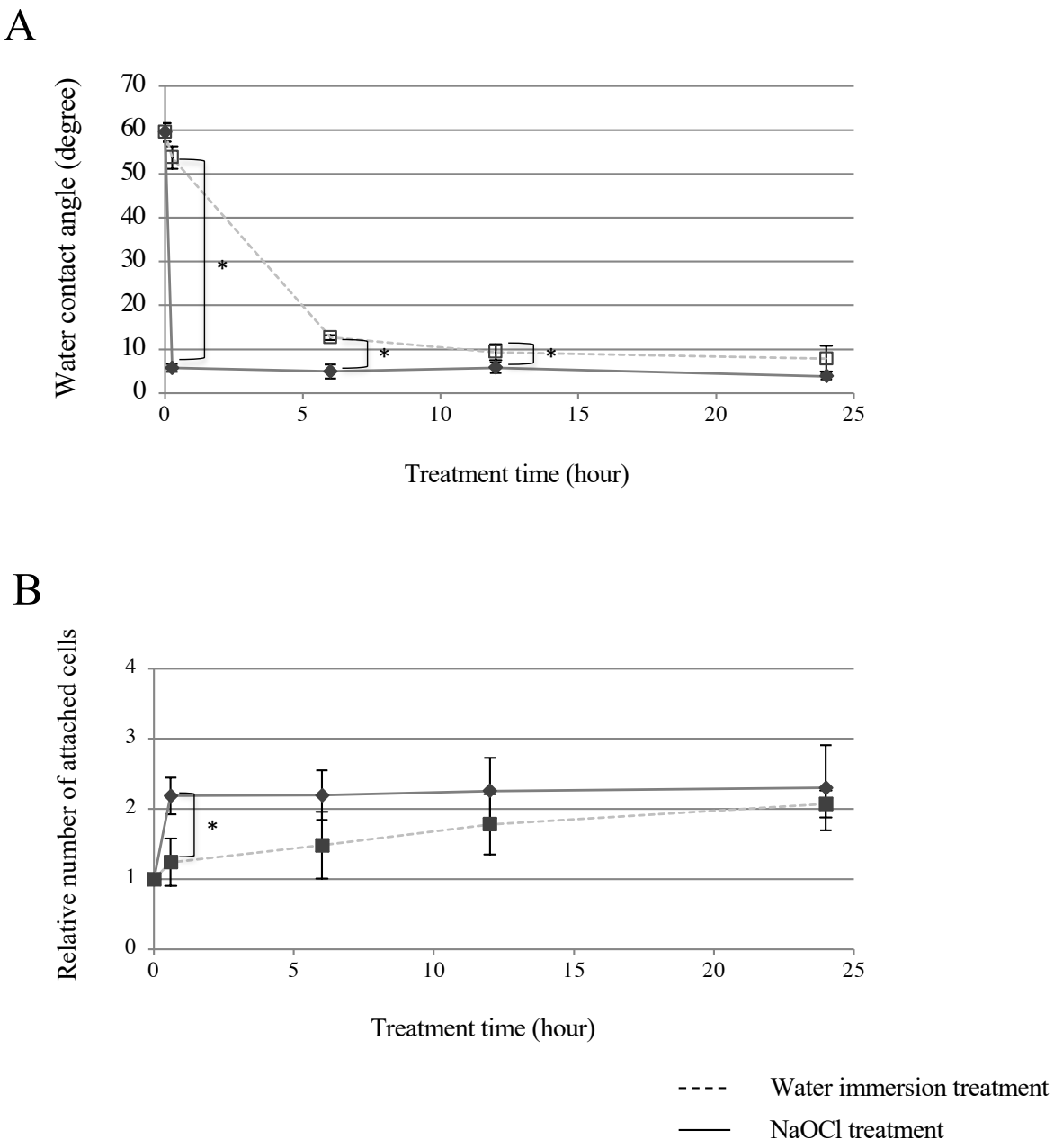

Figure. 11 (A) Water contact angle was obtained from image analysis of the 4 μl water droplets. Date are shown as mean ±SD (n = 3) (B) The variation of relative number of cells attached to the titanium surface with the treatment time. Date are shown as mean ±SD (n = 4). Paired *t*-test ＊$p < 0.05$, indicating a significant difference. This figure was published in Ichioka et al. (2021), Copyright 2021 The Japanese Society for Dental Materials and Devices, and reused with permission from the journal.

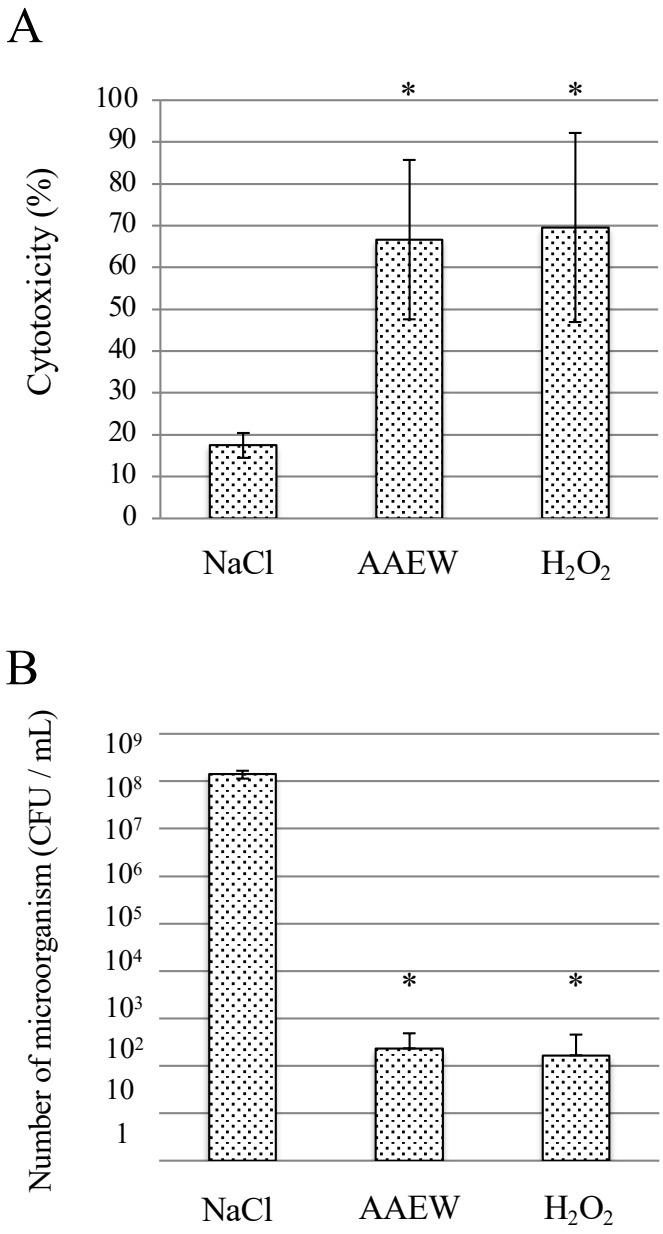

Figure 12. Cytotoxicity effects towards hBMSCs and bactericidal effect for *S. gordonii.* (A) Trypan blue test for cytotoxicity towards hBMSCs (n = 4). (B) Bactericidal effects for *S. gordonii* (n = 3). *Indicate significant difference in comparison with NaCl ($p< 0.05$). This figure was published in Ichioka et al. (2020) and reused with permission from the journal.

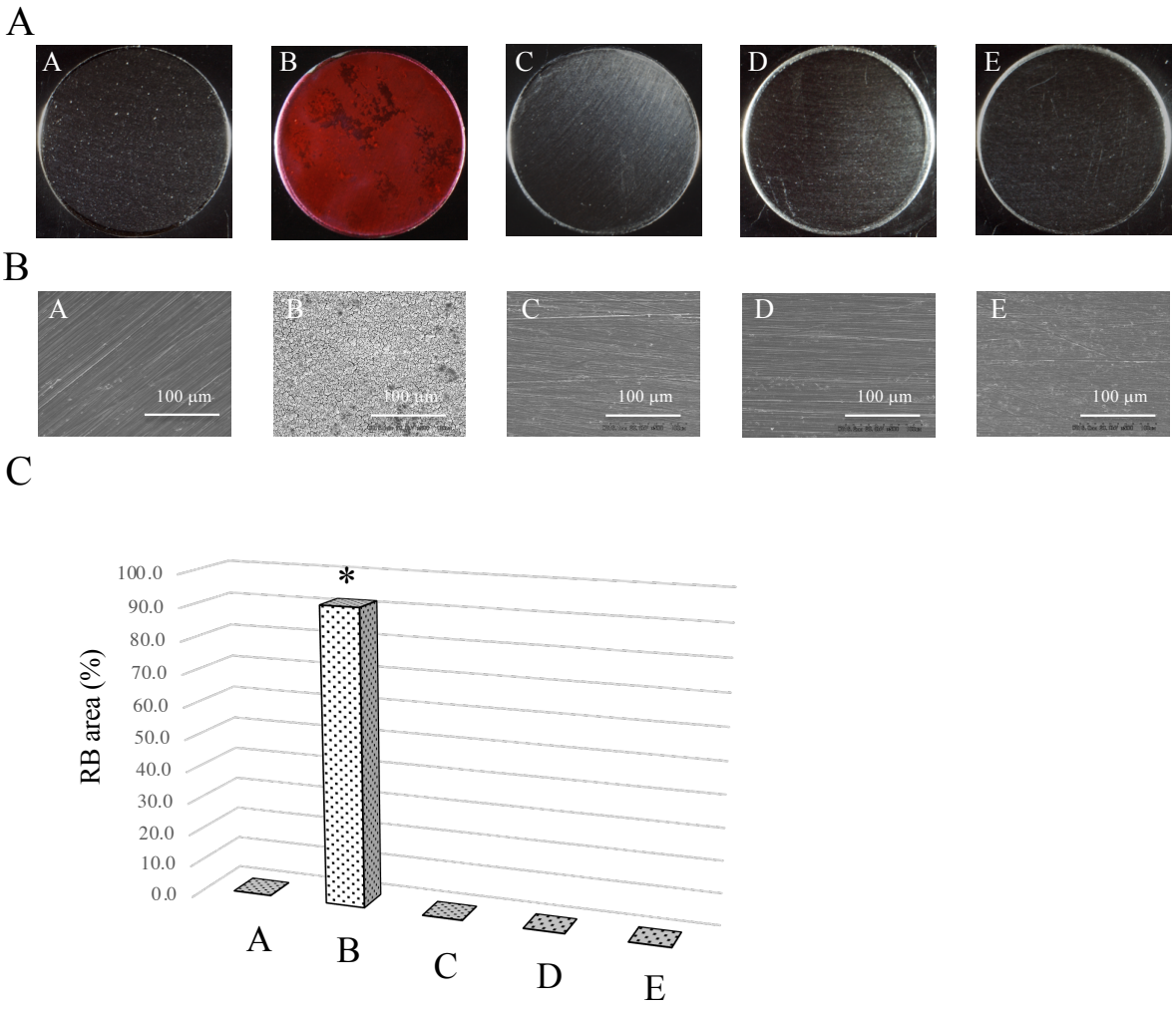

Figure 13. Evaluation of biofilm removal from titanium compared with As-polished surface: (a) As-polished; (b) Biofilm-contaminated; (c) Air + NaCl; (d) Air + AAEW; (e) Air + H_2O_2. (A) Light microscopy images of As-polished and residual biofilm (RB) areas in different groups. (B) SEM images titanium group surfaces. Bar indicates 100 µm, magnification × 500. (C) Mean (± SD) RB areas on each titanium surface (n = 4 / group), *p <0.001 vs As-polished and each treatment group. The contents in this figure were published in Ichioka et al. (2020) and reused with permission from the journal.

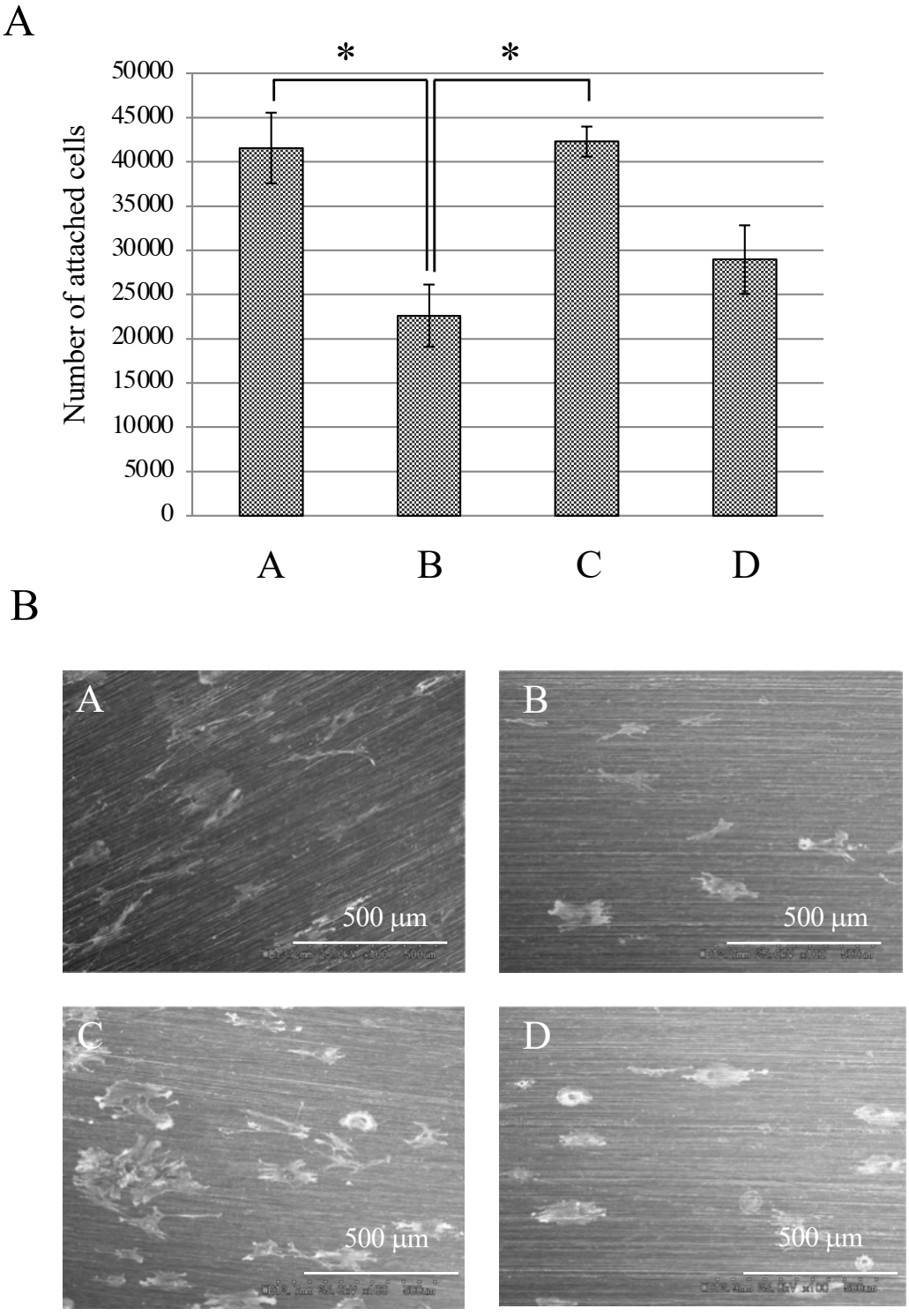

Figure 14. Initial cell attachment on titanium surfaces: (a) As-polished; (b) Air + NaCl; (c) Air + AAEW; (d) Air + H_2O_2. (A) Number of attached hBMSCs. Bars indicate the mean ± SD (n = 3). *p< 0.05 (B) SEM images of cell density on each of the conditioned titanium surface groups. Bar indicates 500 μm, magnification × 100. This figure was published in Ichioka et al. (2020) and reused with permission from the journal.

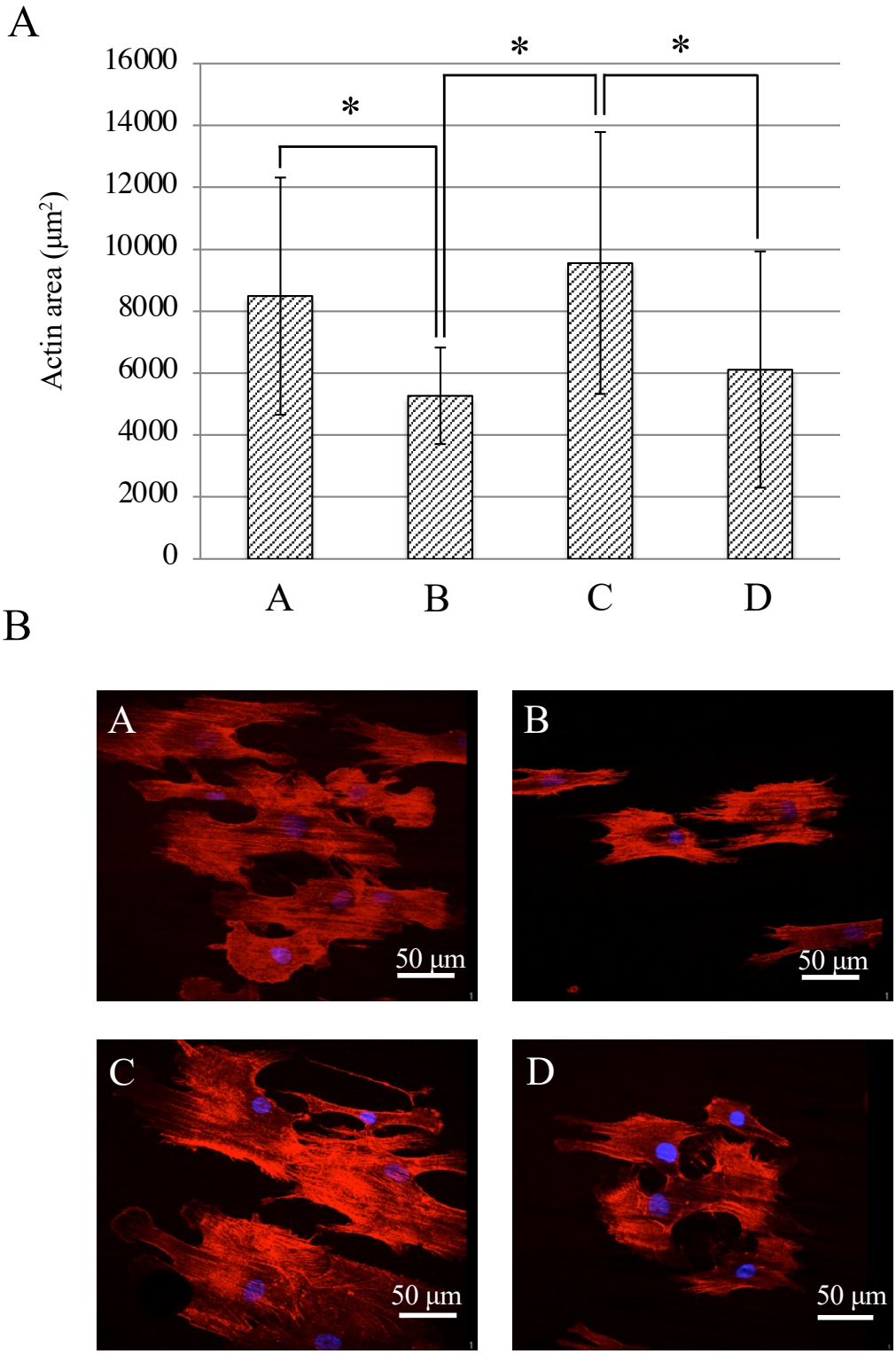

Figure 15. Initial hBMSC spreading after seeding on titanium surfaces: (a) As-polished; (b) Air + NaCl; (c) Air + AAEW; (d) Air + H_2O_2. (A) Cell morphometric evaluations performed using the images. Bars indicate the mean ± SD (n = 25), *p< 0.05 (B) Confocal laser scanning microscopy images of hBMSCs. Representative confocal microscopic images of cells dual-stained with rhodamine phalloidin to identify actin filaments (red) and DAPI for nuclei (blue). This figure was published in Ichioka et al. (2020) and reused with permission from the journal.

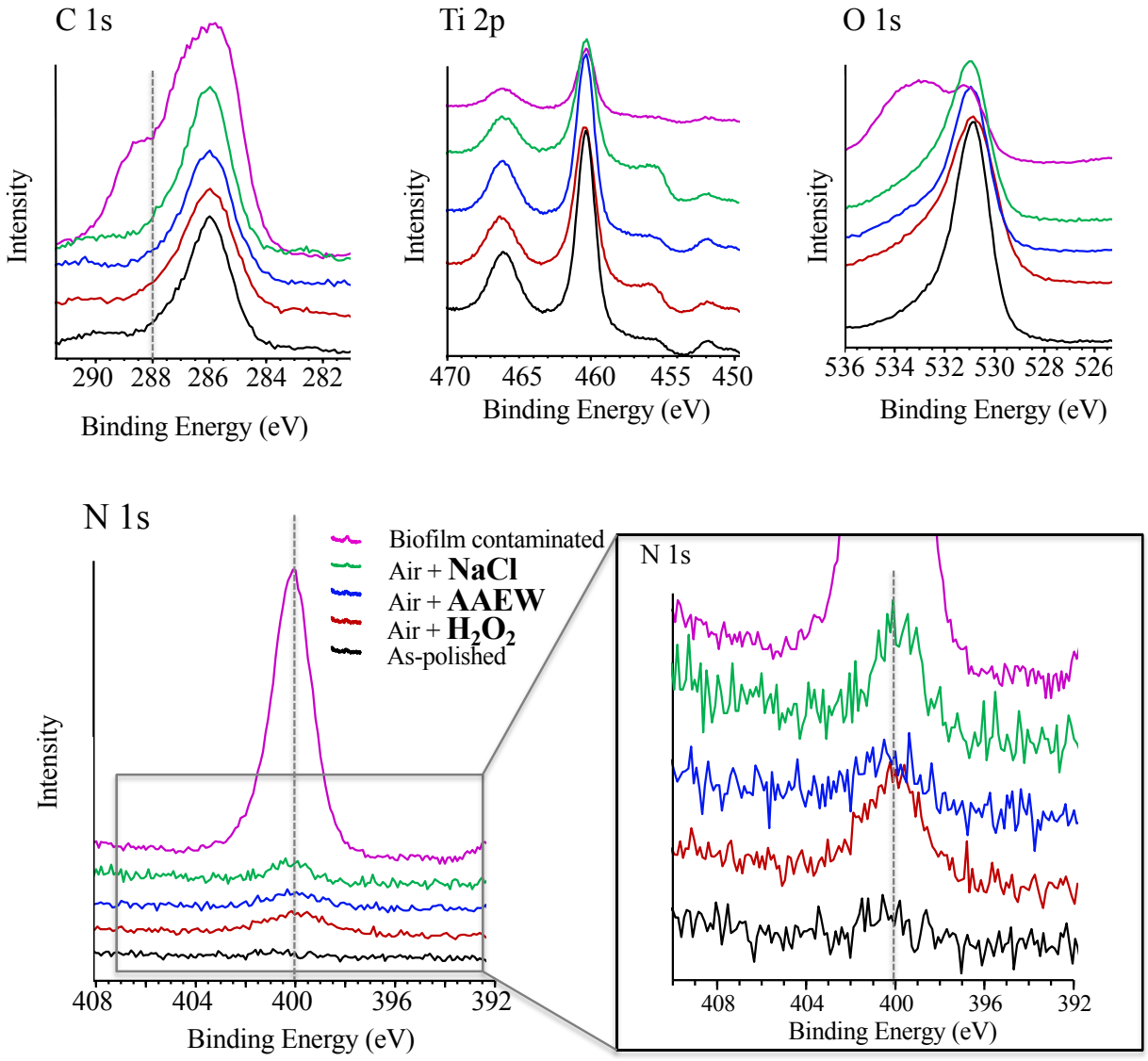

Figure 16. Analysis of surface chemical properties. Ti 2p, C 1s, O 1s, and N 1s spectra obtained from each conditioned titanium surface. Peak intensity was evaluated by the height from the baseline of each spectrum. This figure was published in Ichioka et al. (2020) and reused with permission from the journal.

(A) Aliphatic saturated hydrocarbons (alkanes)

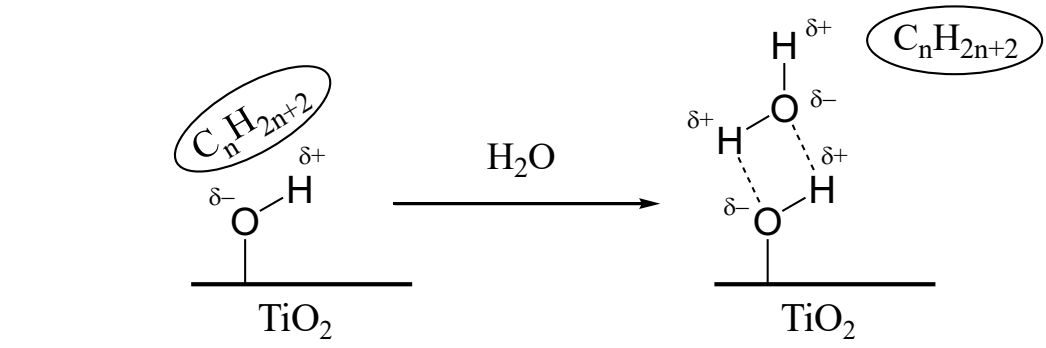

(B) Amine

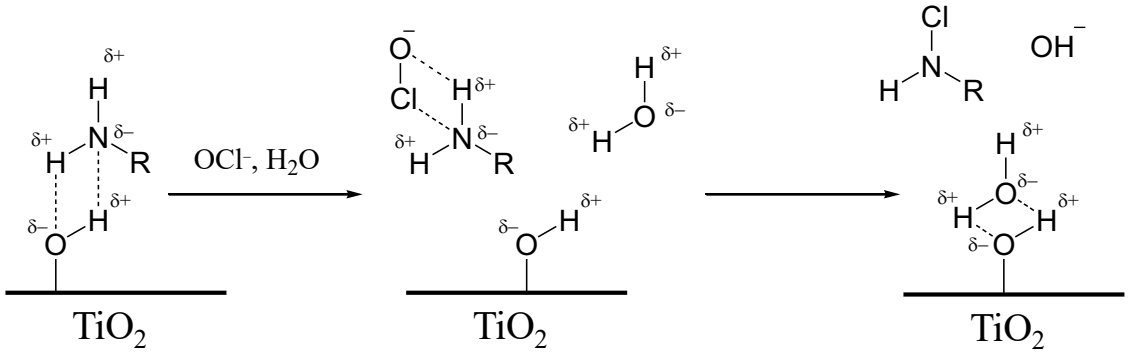

(C) Aldehyde

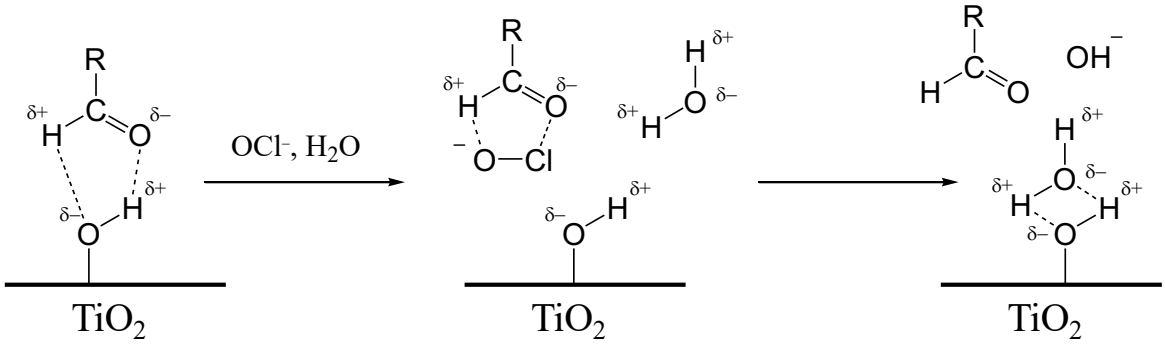

Figure 17. The process for desorption of VOCs or ONDs from the contaminated titanium surface. This figure was published in Ichioka et al. (2021), Copyright 2021 The Japanese Society for Dental Materials and Devices, and reused with permission from the journal.

Figure legends

Figure. 1 Chemical surface treatments employed in study I.

Figure. 2 Mechanical and chemical surface treatments employed in study II.

Figure. 3 (A) The image of 4 μl water droplets on the each titanium surface. (B) The water contact angle was obtained from image analysis of the 4 μl water droplets. Date are shown as mean ± SD (n = 5). *Indicate significant difference in comparison with Untreated ($p< 0.05$).

Figure. 4 The amount of adsorbed Collagen I on the each titanium surfaces.

Fluorescence intensity was obtained by measuring the mean gray value of CLSM images using IMAGE-J software. Data are shown as the mean ± SD (n = 3). *: $p< 0.05$ for significance.

Figure. 5 (A) The relative number of attached hBMSCs 4 hours after seeding on the titanium surfaces measured with a hemocytometer. Data are shown as the mean ± SD (n = 4). *Indicate significant difference in comparison with Untreated ($p< 0.05$). (B) Cell density image (magnification x40) on the titanium surfaces as observed by SEM.

Figure. 6 (A) Fluorescent images of the hBMSCs on the titanium disks. (B) Cytomorphometric evaluations for the area, Perimeter and Feret's diameter of the cells. Data are shown as the mean ± SD (n = 5). *: $p< 0.05$ for significance.

Figure. 7 Ti 2p, C 1s and N 1s spectra obtained from the same specimens at before and after immersion in deionized water.

Figure. 8 Percent area of hydroxyl groups in O 1s spectra at before and after immersion in deionized water.

Figure. 9 Ti 2p, C 1s and N 1s spectra obtained from the same specimens at before and after immersion in NaOCl solution.

Figure. 10 Percent area of hydroxyl groups in O 1s spectra at before and after immersion in NaOCl solution.

Figure. 11 (A) Water contact angle was obtained from image analysis of the 4 ml water droplets. Date are shown as mean ±SD (n = 3) (B) The variation of relative number of cells attached to the titanium surface with the treatment time. Date are shown as mean ±SD (n = 4). Paired *t*-test $* p< 0.05$, indicating a significant difference.

Figure 12. Cytotoxicity effects towards hBMSCs and bactericidal effect for *S. gordonii*. (A) Trypan blue test for cytotoxicity towards hBMSCs (n = 4). (B) Bactericidal effects for *S. gordonii* (n = 3). *Indicate significant difference in comparison with NaCl ($p< 0.05$).

Figure 13. Evaluation of biofilm removal from titanium compared with As-polished surface: (a) As-polished; (b) Biofilm-contaminated; (c) Air + NaCl; (d) Air + AAEW; (e) Air + H_2O_2.

(A) Light microscopy images of As-polished and residual biofilm (RB) areas in different groups. (B) SEM images titanium group surfaces. Bar indicates 100 μm, magnification × 500. (C) Mean (± SD) RB areas on each titanium surface (n = 4 / group), *p <0.001 vs As-polished and each treatment group.

Figure 14. Initial cell attachment on titanium surfaces: (a) As-polished; (b) Air + NaCl; (c) Air + AAEW; (d) Air + H_2O_2. (A) Number of attached hBMSCs. Bars indicate the mean ± SD (n = 3). *p< 0.05 (B) SEM images of cell density on each of the conditioned titanium surface groups. Bar indicates 500 μm, magnification × 100.

Figure 15. Initial hBMSC spreading after seeding on titanium surfaces: (a) As-polished; (b) Air + NaCl; (c) Air + AAEW; (d) Air + H_2O_2. (A) Cell morphometric evaluations performed using the images. Bars indicate the mean ± SD (n = 25), *p< 0.05 (B) Confocal laser scanning microscopy images of hBMSCs. Representative confocal microscopic images of cells dual-stained with rhodamine phalloidin to identify actin filaments (red) and DAPI for nuclei (blue).

Figure 16. Analysis of surface chemical properties. Ti 2p, C 1s, O 1s, and N 1s spectra obtained from each conditioned titanium surface. Peak intensity was evaluated by the height from the baseline of each spectrum.

Figure 17. The process for desorption of VOCs or ONDs from the contaminated titanium surface.